



Gruneisen parameter and thermal expansion near magnetic quantum critical points in itinerant electron systems

著者	Watanabe Shinji, Miyake Kazumasa
journal or publication title	Physical Review B
page range	035108-1-035108-25
year	2019-01-03
その他のタイトル	Gruneisen Parameter and Thermal Expansion near Magnetic Quantum Critical Points in Itinerant Electron Systems
URL	http://hdl.handle.net/10228/00007061


doi: [info:doi/10.1103/PhysRevB.99.035108](https://doi.org/10.1103/PhysRevB.99.035108)

Grüneisen parameter and thermal expansion near magnetic quantum critical points in itinerant electron systems

Shinji Watanabe¹ and Kazumasa Miyake²

¹*Department of Basic Sciences, Kyushu Institute of Technology, Kitakyushu, Fukuoka 804-8550, Japan*

²*Center for Advanced High Magnetic Field Science, Osaka University, Toyonaka, Osaka 560-0043, Japan*

 (Received 17 February 2018; revised manuscript received 10 December 2018; published 3 January 2019)

Complete expressions of the thermal-expansion coefficient α and the Grüneisen parameter Γ are derived on the basis of the self-consistent renormalization (SCR) theory. By considering the zero point as well as thermal spin fluctuation under the stationary condition, the specific heat for each class of the magnetic quantum critical point (QCP) specified by the dynamical exponent $z = 3$ [ferromagnetism (FM)] and $z = 2$ [antiferromagnetism (AFM)] and the spatial dimension ($d = 3$ and 2) is shown to be expressed as $C_V = C_a - C_b$, where C_a is dominant at low temperatures, reproducing the past SCR criticality endorsed by the renormalization group theory. Starting from the explicit form of the entropy and using the Maxwell relation, $\alpha = \alpha_a + \alpha_b$ (with α_a and α_b being related to C_a and C_b , respectively) is derived, which is proven to be equivalent to α derived from the free energy. The temperature-dependent coefficient found to exist in α_b , which is dominant at low temperatures, contributes to the crossover from the quantum-critical regime to the Curie-Weiss regime. For sufficiently low temperatures, the thermal-expansion coefficient at the QCP behaves as $\alpha \approx \alpha_b \sim T^{1/3}$ (3D FM), $T^{1/2}$ (3D AFM), $-\ln T$ (2D FM), and $-\ln(-\ln T)/\ln(-\frac{T}{\ln T})$ (2D AFM). Based on these correctly calculated C_V and α , Grüneisen parameter $\Gamma = \Gamma_a + \Gamma_b$ is derived, where Γ_a and Γ_b contain α_a and α_b , respectively. The inverse susceptibility (renormalized by the mode-mode coupling of spin fluctuations) coupled to the volume V in Γ_b gives rise to the divergence of Γ at the QCP for each class even though the characteristic energy scale of spin fluctuation T_0 is finite at the QCP, which gives a finite contribution in $\Gamma_a = -\frac{V}{T_0}(\frac{\partial T_0}{\partial V})_{T=0}$. For $T \ll T_0$, the Grüneisen parameter at the QCP behaves as $\Gamma \approx \Gamma_b \sim -T^{-2/3}/\ln T$ (3D FM), $T^{-1/2}/(\text{const.} - T^{1/2})$ (3D AFM), $-T^{-2/3} \ln T$ (2D FM), and $\ln(-\ln T)/[T \ln T \ln(-\frac{T}{\ln T})]$ (2D AFM). General properties of α and Γ including their signs as well as the relation to T_0 and the Kondo temperature in temperature-pressure phase diagrams of Ce- and Yb-based heavy electron systems are discussed.

DOI: [10.1103/PhysRevB.99.035108](https://doi.org/10.1103/PhysRevB.99.035108)

I. INTRODUCTION

Quantum critical phenomena in itinerant electron systems have attracted much attention in condensed matter physics. When the transition temperature to the magnetically ordered phase is suppressed continuously to absolute zero by tuning a control parameter of materials such as pressure, magnetic field, and chemical substitution, the quantum critical point (QCP) is realized. Near the QCP, enhanced magnetic fluctuation causes a non-Fermi-liquid behavior in physical quantities, which is referred to as quantum critical phenomena.

The self-consistent renormalization (SCR) theory of spin fluctuation has been developed by Moriya and Kawabata in 1973 [1,2]. The SCR theory succeeded in explaining not only the Curie-Weiss behavior but also quantum critical behavior at low temperatures in magnetic susceptibility, which are caused by spin fluctuation in nearly ferromagnetic metals [3,4]. The spin fluctuation has been revealed to cause a non-Fermi-liquid behavior in the specific heat [5] and the resistivity [6] in nearly ferromagnetic metals and also in nearly antiferromagnetic metals [3].

The quantum critical phenomena have been studied by the renormalization-group (RG) theory by Hertz in 1976 [7] and reexamined by Millis in 1993 [8], which has explained low-temperature properties of physical quantities in the

vicinity of the QCP. The RG theory has been shown to yield the same critical exponents [9] as those found in the SCR theory [10–14].

The magnetovolume effect in nearly ferromagnetic metals has been studied by Moriya and Usami in 1980 [15]. They discussed the effect of spin fluctuation on the thermal expansion and the effect was also studied in nearly antiferromagnetic metals [13]. In 1997, Kambe *et al.* analyzed the thermal-expansion coefficient and the Grüneisen parameter observed in $\text{Ce}_{1-x}\text{La}_x\text{Ru}_2\text{Si}_2$ by using the SCR theory and the RG theory and pointed out a possibility that the Grüneisen parameter diverges at the QCP [16]. In 2003, by using the scaling hypothesis and the RG theory, Zhu *et al.* evaluated a critical part of the thermal expansion coefficient. By taking the ratio to the critical part of the specific heat, they evaluated the critical part of the Grüneisen parameter, which actually diverges at the QCP [17,18]. Experimentally, in CeNi_2Ge_2 , which is located closely to the three-dimensional (3D) AFM QCP, the divergence of the Grüneisen parameter has been observed [19]. Divergence of the Grüneisen parameter has also been observed in $\text{CeIn}_{3-x}\text{Sn}_x$ ($x = 0.65$) [20] and in $\text{CeRhIn}_{5-x}\text{Sn}_x$ ($x = 0.48$) [21], where the 3D AFM order is suppressed by the chemical doping.

It is well known that if the system is dominated by a single energy scale T^* , the entropy is expressed as a scaled form

$S = k_B f(T/T^*)$, where k_B is the Boltzmann constant and T is temperature, so that the Grüneisen parameter is given by $\Gamma = -\frac{V}{T^*} \left(\frac{\partial T^*}{\partial V} \right)_S$ with V being the volume [22–24]. Normal metal with the Fermi temperature is known to be the case and lattice system with the Debye temperature where acoustic phonons give the dominant contribution is also the case. The expression of Γ suggests that if T^* becomes zero with nonvanishing $(\partial T^*/\partial V)_S$, the Grüneisen parameter diverges.

On the other hand, in the SCR theory, there exists the characteristic energy scale of spin fluctuation T_0 , which is known to be finite even at the QCP in general [3]. It is also known that the magnetic correlation length diverges at the QCP, the inverse of which gives the zero characteristic scale. Hence, it is interesting to clarify how these quantities affect Γ at the FM QCP and also AFM QCP. This requires theoretical study to clarify how the Grüneisen parameter behaves at the QCP in the SCR theory.

An advantageous point of the SCR theory is that it describes not only the quantum critical behavior in the vicinity of the QCP, but also the Curie-Weiss behavior at higher temperatures in the magnetic susceptibility in a unified way [3]. The crossover from the quantum-critical regime to the high-temperature (Curie-Weiss) regime for the other physical quantities such as the specific heat and the resistivity can also be calculated [3,25,26].

So far, critical parts of the thermal-expansion coefficient α and the Grüneisen parameter Γ were reported by the RG theory [17,18]. It seems important to clarify their complete expressions with not only the critical part but also noncritical part including their coefficients of the temperature-dependent terms in the SCR theory. In many cases the critical part is observed in the very vicinity of the QCP, and in case experimentally accessible temperature does not reach the low-temperature regime, the crossover behavior is usually observed. Hence, it is useful to obtain the complete expressions of α and Γ for comparison with experiments.

In the original SCR theory, the specific heat was calculated with the zero-point spin fluctuation being neglected [10–12]. Taking into account the zero-point spin fluctuation [14,27] as well as the stationary condition of the free energy adequately [27], the specific heat was calculated, which has shown that the dominant contribution to the quantum criticality comes from the thermal spin fluctuation and the critical indices [10–12] endorsed by the RG theory [8,9] do not change.

However, in the calculation of the thermal-expansion coefficient and the Grüneisen parameter in the SCR theory, the zero-point spin fluctuation as well as the stationary condition of the free energy should be taken into account correctly, which has not been addressed in Refs. [15,16]. Takahashi considered these effects in the extended SCR theory by introducing the conservation law of the total spin-fluctuation amplitude and discussed the magnetovolume effect [28].

In this paper we derive the thermal expansion coefficient α and the Grüneisen parameter Γ in the *complete* framework of the original SCR theory. By taking into account zero-point spin fluctuation as well as the stationary condition of the free energy correctly, we reexamine the specific heat C_V near the ferromagnetic (FM) QCP and the antiferromagnetic (AFM) QCP in three spatial dimensions ($d = 3$) and two spatial dimensions ($d = 2$). Then we derive the thermal expansion

coefficient α for each class starting from the entropy, which is proven to be equivalent to that obtained from the explicit form of the free energy with the use of the stationary condition in the SCR theory. On the basis of these correctly calculated C_V and α , we obtain Γ . By performing analytical and numerical calculations of C_V , α , and Γ near the magnetic QCP, their quantum-critical properties are clarified.

We find that the temperature dependent coefficient exists in the expressions of $\alpha(T)$ and $\Gamma(T)$, which has not been reported in the past RG studies [17,18]. Furthermore, the complete expressions of $\alpha(T)$ and $\Gamma(T)$ clarify the crossover from the quantum-critical regime at low temperatures to the Curie-Weiss regime at higher temperatures for each class of the QCP. Then we give the answers to the following questions: (1) What is the relation to the divergence of Γ at the QCP shown by the RG theory? (2) How to reconcile with finite T_0 at the QCP in the SCR theory? (3) What is the relation to the Moriya-Usami theory?

The organization of this paper is as follows: In Sec. II the definitions of the thermal-expansion coefficient and the Grüneisen parameter are explained by introducing thermodynamically equivalent expressions. In Sec. III the SCR theory is outlined and the properties of the specific heat near the QCP are summarized. In Sec. IV the Grüneisen parameter is derived from the entropy in the SCR theory. In Sec. V the thermal-expansion coefficient near the QCP is derived from the entropy and the free energy, respectively, in the SCR theory and equivalence of both the results is proven. In Secs. VI, VII, and VIII, results of numerical calculations of the thermal expansion coefficient and the Grüneisen parameter near the QCP for each class are analyzed, respectively. Section IX is devoted to discussions by comparing the present theory with other theories and experiments. In Sec. X the paper is summarized. From Secs. II to VIII we concentrate on the electronic Grüneisen parameter relevant for low temperatures where lattice degrees of freedom give minor contributions. In Sec. IX the general case including phonons is discussed.

II. THERMAL-EXPANSION COEFFICIENT AND GRÜNEISEN PARAMETER

In this section the definitions of the thermal-expansion coefficient α and the Grüneisen parameter Γ are summarized. The equivalent expressions of α and Γ are also derived for the use in discussions in the forthcoming sections.

A. Thermal-expansion coefficient

The thermal-expansion coefficient is defined as

$$\alpha = \frac{1}{V} \left(\frac{\partial V}{\partial T} \right)_P, \quad (1)$$

where P is the pressure. By using the relation

$$\left(\frac{\partial V}{\partial T} \right)_P = - \frac{\left(\frac{\partial P}{\partial T} \right)_V}{\left(\frac{\partial P}{\partial V} \right)_T}, \quad (2)$$

Eq. (1) is expressed as

$$\alpha = \kappa_T \left(\frac{\partial P}{\partial T} \right)_V, \quad (3)$$

where the isothermal compressibility κ_T is defined as

$$\kappa_T = -\frac{1}{V} \left(\frac{\partial V}{\partial P} \right)_T. \quad (4)$$

On the other hand, by using the Maxwell relation $(\partial V/\partial T)_P = -(\partial S/\partial P)_T$ in Eq. (1), α can be expressed as

$$\alpha = -\frac{1}{V} \left(\frac{\partial S}{\partial P} \right)_T. \quad (5)$$

B. Grüneisen parameter

The Grüneisen parameter Γ is defined by

$$\Gamma = \frac{\alpha V}{C_V \kappa_T}, \quad (6)$$

where C_V is the specific heat at a constant volume

$$C_V = T \left(\frac{\partial S}{\partial T} \right)_V. \quad (7)$$

With the use of Eq. (5) for α in Eq. (6), the Grüneisen parameter Γ is expressed as follows:

$$\begin{aligned} \Gamma &= -\frac{\partial(S, T)}{\partial(P, T)} \frac{1}{T} \frac{(-V)}{\frac{\partial(S, V)}{\partial(T, V)} \frac{\partial(V, T)}{\partial(P, T)}} \\ &= -\frac{V}{T} \frac{\partial(S, T)}{\partial(S, V)} = -\frac{V}{T} \left(\frac{\partial T}{\partial V} \right)_S. \end{aligned} \quad (8)$$

If the entropy is expressed as $S = k_B S(T/T^*)$ with a single characteristic temperature scale T^* as in the Fermi-liquid region of metals, $(\partial T/\partial V)_S$ is given in a form as

$$\left(\frac{\partial T}{\partial V} \right)_S = \frac{T}{T^*} \left(\frac{\partial T^*}{\partial V} \right)_S. \quad (9)$$

Then the Grüneisen parameter Γ is expressed as a conventional form as [23,29]

$$\Gamma = -\left(\frac{\partial \ln T^*}{\partial \ln V} \right)_S. \quad (10)$$

III. SCR THEORY

In this section the self-consistent renormalization (SCR) theory of spin fluctuation is outlined. By taking into account the zero point as well as thermal spin fluctuation under consideration of the stationary condition of the SCR theory, the specific heat near the magnetic QCP is reexamined. Hereafter the energy units are taken as $\hbar = 1$ and $k_B = 1$ unless otherwise noted.

A. Formulation of the SCR theory

The action of the itinerant electrons with Coulomb interaction is expressed in the form of the Ginzburg-Landau-Wilson functional

$$\begin{aligned} \Phi[\varphi] &= \frac{1}{2} \sum_{\bar{q}} \Omega_2(\bar{q}) \varphi(\bar{q}) \varphi(-\bar{q}) + \sum_{\bar{q}_1, \bar{q}_2, \bar{q}_3, \bar{q}_4} \Omega_4(\bar{q}_1, \bar{q}_2, \bar{q}_3, \bar{q}_4) \\ &\quad \times \varphi(\bar{q}_1) \varphi(\bar{q}_2) \varphi(\bar{q}_3) \varphi(\bar{q}_4) \delta \left(\sum_{i=1}^4 \bar{q}_i \right), \end{aligned} \quad (11)$$

which can be derived from the Hamiltonian via the Stratonovich-Hubbard transformation applied to the on-site Coulomb interaction term [7]. Hence, Eq. (11) describes the action for isotropic spin space [30]. Here \bar{q} is an abbreviation for $\bar{q} \equiv (\mathbf{q}, i\omega_l)$ where $\omega_l = 2\pi l/T$ with l being an integer. Since long wavelength $|\mathbf{q}| \ll q_c$ around the magnetically ordered vector \mathbf{Q} and low frequency $|\omega| \ll \omega_c$ regions play the dominant role in the critical phenomena with q_c and ω_c being the cutoffs for momentum and frequency, respectively, Ω_i for $i = 2, 4$ are expanded for q and ω around $(\mathbf{Q}, 0)$:

$$\Omega_2(\mathbf{q}, i\omega_l) \approx \frac{\eta_0 + Aq^2 + C_q |\omega_l|}{N_F}, \quad (12)$$

where C_q is defined as $C_q \equiv C/q^{z-2}$ with z being the dynamical exponent (e.g., $z = 3$ for ferromagnetism and $z = 2$ for antiferromagnetism) and N_F is the density of states at the Fermi level, and $\Omega_4(\bar{q}_1, \bar{q}_2, \bar{q}_3, \bar{q}_4) \approx v_4/(\beta N)$ with $\beta \equiv 1/T$.

To construct the effective action for the best Gaussian, taking account of the mode-mode coupling effects up to the fourth order in $\Phi[\varphi]$, we employ the Feynman's inequality [32] on the free energy:

$$F \leq F_{\text{eff}} + T \langle \Phi - \Phi_{\text{eff}} \rangle_{\text{eff}} \equiv \tilde{F}(\eta). \quad (13)$$

Here the effective action Φ_{eff} is parametrized as

$$\Phi_{\text{eff}}[\varphi] = \frac{1}{2} \sum_l \sum_q \frac{\eta + Aq^2 + C_q |\omega_l|}{N_F} |\varphi(q, i\omega_l)|^2, \quad (14)$$

where η expresses the effect of the mode-mode coupling of spin fluctuations and parametrizes the closeness to the quantum criticality. In Eq. (13), $\langle \dots \rangle_{\text{eff}}$ denotes the statistical average taken by the weight $\exp(-\Phi_{\text{eff}}[\varphi])$ and F_{eff} is given by

$$F_{\text{eff}} = -T \ln \int \mathcal{D}\varphi \exp(-\Phi_{\text{eff}}[\varphi]). \quad (15)$$

By optimal condition $\frac{d\tilde{F}(\eta)}{d\eta} = 0$, the self-consistent renormalization (SCR) equation for η is given by

$$\frac{\eta_0 - \eta}{2N_F} + \frac{6v_4}{N} \langle \varphi^2 \rangle_{\text{eff}} = 0, \quad (16)$$

where spin fluctuation $\langle \varphi^2 \rangle_{\text{eff}}$ is defined as

$$\langle \varphi^2 \rangle_{\text{eff}} = T \sum_q \sum_l \frac{N_F}{\eta + Aq^2 + C_q |\omega_l|}. \quad (17)$$

Here $\langle \varphi^2 \rangle_{\text{eff}}$ consists of the quantum (zero-point) fluctuation $\langle \varphi^2 \rangle_{\text{zero}}$ and thermal fluctuation $\langle \varphi^2 \rangle_{\text{th}}$ as

$$\langle \varphi^2 \rangle_{\text{eff}} = \langle \varphi^2 \rangle_{\text{zero}} + \langle \varphi^2 \rangle_{\text{th}}, \quad (18)$$

where $\langle \varphi^2 \rangle_{\text{zero}}$ and $\langle \varphi^2 \rangle_{\text{th}}$ are expressed as

$$\langle \varphi^2 \rangle_{\text{zero}} = \frac{N_F}{\pi} \sum_q \frac{1}{C_q} \int_0^{\omega_c} d\omega \frac{\omega}{\Gamma_q^2 + \omega^2}, \quad (19)$$

$$\langle \varphi^2 \rangle_{\text{th}} = \frac{N_F}{\pi} \sum_q \frac{2}{C_q} \int_0^{\omega_c} d\omega \frac{1}{e^{\beta\omega} - 1} \frac{\omega}{\Gamma_q^2 + \omega^2}, \quad (20)$$

respectively. Here Γ_q is defined by $\Gamma_q \equiv (\eta + Aq^2)/C_q$.

From Eq. (14), the dynamical magnetic susceptibility is given by

$$\chi_{\mathbf{Q}}(q, \omega) = \frac{N_{\text{F}}}{\eta + Aq^2 - iC_q\omega}, \quad (21)$$

where \mathbf{Q} is the wave number vector of the magnetically ordered phase (e.g., $\mathbf{Q} = \mathbf{0}$ for ferromagnetism and $\mathbf{Q} \neq \mathbf{0}$ for antiferromagnetism).

The free energy \tilde{F} defined by Eq. (13) is expressed as

$$\begin{aligned} \tilde{F} = & \frac{1}{\pi} \sum_q \int_0^{\omega_c} d\omega \frac{\Gamma_q}{\omega^2 + \Gamma_q^2} \left\{ \frac{\omega}{2} + T \ln(1 - e^{-\frac{\omega}{T}}) \right\} \\ & + \frac{\eta_0 - \eta}{2N_{\text{F}}} \langle \varphi^2 \rangle_{\text{eff}} + \frac{3v_4}{N} \langle \varphi^2 \rangle_{\text{eff}}^2 - \frac{1}{\pi} \sum_q \frac{\pi\omega_c}{4}. \end{aligned} \quad (22)$$

Here, let us define dimensionless parameters for η ,

$$y \equiv \frac{\eta}{Aq_{\text{B}}^2} \quad (23)$$

and the wave number $x \equiv q/q_{\text{B}}$ with q_{B} being the wave number of the Brillouin zone. Thus, Γ_q is expressed as

$$\Gamma_q = 2\pi T_0 x^{z-2} (y + x^2), \quad (24)$$

where the characteristic temperature of spin fluctuation is defined as

$$T_0 \equiv \frac{Aq_{\text{B}}^2}{2\pi C_{q_{\text{B}}}}. \quad (25)$$

Near the QCP, quantum spin fluctuation $\langle \varphi^2 \rangle_{\text{zero}}$ is calculated [13] for the cases above and just at the upper critical dimension 4, respectively, as

$$\langle \varphi^2 \rangle_{\text{zero}} = Nd \frac{T_0}{2T_{\text{A}}} \begin{cases} C_1 - C_2 y + \dots, & \text{for } d+z > 4, \\ C_1 + y \ln y - C_2 y + \dots, & \text{for } d+z = 4, \end{cases} \quad (26)$$

where T_{A} is defined as

$$T_{\text{A}} \equiv \frac{Aq_{\text{B}}^2}{2N_{\text{F}}}. \quad (27)$$

The constants C_1 and C_2 are given by

$$\begin{aligned} C_1 = & \int_0^{x_c} dx x^{d+z-3} \ln \left| \frac{\omega_c^2 T_0 + x^{2z}}{x^{2z}} \right|, \quad (28) \\ C_2 = & \begin{cases} 2 \int_0^{x_c} dx x^{d+z-5} \frac{\omega_c^2 T_0}{\omega_c^2 T_0 + x^{2z}}, & \text{for } d+z > 4, \\ 1 + \ln x_c^2 - \frac{1}{2} \ln \left| \frac{\omega_c^2 T_0 + x_c^4}{\omega_c^2 T_0} \right|, & \text{for } d+z = 4, \end{cases} \end{aligned} \quad (29)$$

respectively. Here the cut off of the wave number is set to be q_c in the q integration, which is expressed as $x_c \equiv \frac{q_c}{q_{\text{B}}}$ in the dimensionless scaled form and ω_{cT} is defined as $\omega_{cT} \equiv \frac{\omega_c}{2\pi T}$. The thermal spin fluctuation $\langle \varphi^2 \rangle_{\text{th}}$ is calculated as

$$\langle \varphi^2 \rangle_{\text{th}} = Nd \frac{T_0}{T_{\text{A}}} \int_0^{x_c} dx x^{d+z-3} \left\{ \ln u - \frac{1}{2u} - \psi(u) \right\}, \quad (30)$$

where $\psi(u)$ is the digamma function with u defined as

$$u \equiv \frac{\Gamma_q}{2\pi T} = \frac{x^{z-2}(y + x^2)}{t}. \quad (31)$$

Here t is defined as the dimensionless scaled temperature

$$t \equiv \frac{T}{T_0}. \quad (32)$$

By substituting Eqs. (26) and (30) into Eq. (18), the SCR equation [Eq. (16)] is written in the scaled form for $d+z > 4$ as [10–12]

$$y = y_0 + \frac{d}{2} y_1 \int_0^{x_c} dx x^{d+z-3} \left\{ \ln u - \frac{1}{2u} - \psi(u) \right\}, \quad (33)$$

and for $d+z = 4$ as [13]

$$y = y_0 + \frac{y_1}{2} \left(y \ln y + d \int_0^{x_c} dx x \left\{ \ln u - \frac{1}{2u} - \psi(u) \right\} \right), \quad (34)$$

where y_0 and y_1 are given by

$$y_0 = \frac{\frac{\eta_0}{Aq_{\text{B}}^2} + 3dv_4 \frac{T_0}{T_{\text{A}}^2} C_1}{1 + 3dv_4 \frac{T_0}{T_{\text{A}}^2} C_2}, \quad (35)$$

$$y_1 = \frac{12v_4 \frac{T_0}{T_{\text{A}}^2}}{1 + 3dv_4 \frac{T_0}{T_{\text{A}}^2} C_2}, \quad (36)$$

respectively. Here, note that y_0 is different from that obtained by substituting η_0 for η on the right-hand side (r.h.s.) of Eq. (23).

The solution of the SCR equation y is proportional to the inverse susceptibility

$$y = \frac{1}{2T_{\text{A}}} \frac{1}{\chi_{\mathbf{Q}}(0, 0)}, \quad (37)$$

which is obtained by substituting Eq. (23) into Eq. (21) with the use of Eq. (27). Numerical solutions of Eqs. (33) and (34) are shown in Figs. 1(a)–1(c) and Fig. 1(d), respectively [10–13]. The t dependencies of y for the paramagnetic region ($y_0 > 0$) and the region where the magnetic order occurs ($y_0 < 0$) and just at the QCP ($y_0 = 0$) are shown. For $y_0 < 0$, $y = 0$ is realized for $t > 0$ in the case of $d = 3$ [see Figs. 1(a) and 1(b)], where the magnetic phase transition takes place at finite temperature, while $y = 0$ is realized only at $t = 0$ for $d = 2$ [see Figs. 1(c) and 1(d)], satisfying the Mermin-Wagner theorem [33]. In each class, the Curie-Weiss behavior $\chi_{\mathbf{Q}}(0, 0) \propto y^{-1} \sim t^{-1}$ appears in the high- t regime [e.g., see $t \gtrsim 0.07$ in Fig. 1(a)]. The quantum critical region appears in the low- t regime at the QCP realized for $y_0 = 0$, whose property in each class is analyzed as follows.

In $d = 3$, the x integral in Eq. (33) converges for $y \rightarrow 0$ and then the solution is obtained as

$$y \propto t^{1+\frac{1}{z}} \quad (38)$$

at the QCP with $y_0 = 0.0$, as shown in Appendix B. This yields $y \sim t^{4/3}$ for the 3D FM QCP ($z = 3$) and $y \sim t^{3/2}$ for the 3D AF QCP ($z = 2$).

In $d = 2$, the x integral in Eq. (33) shows logarithmic divergence for $y \rightarrow 0$. At the FM QCP for $z = 3$, the solution of Eq. (33) is obtained as $y = -\frac{y_1}{12} t \ln t$ (see Appendix C). At the AF QCP for $z = 2$, the solution of Eq. (34) is obtained as $y = -t \frac{\ln(-\ln t)}{2 \ln t}$ (see Appendix D). The criticality $y(\propto \eta)$ for each class is summarized in Table I.

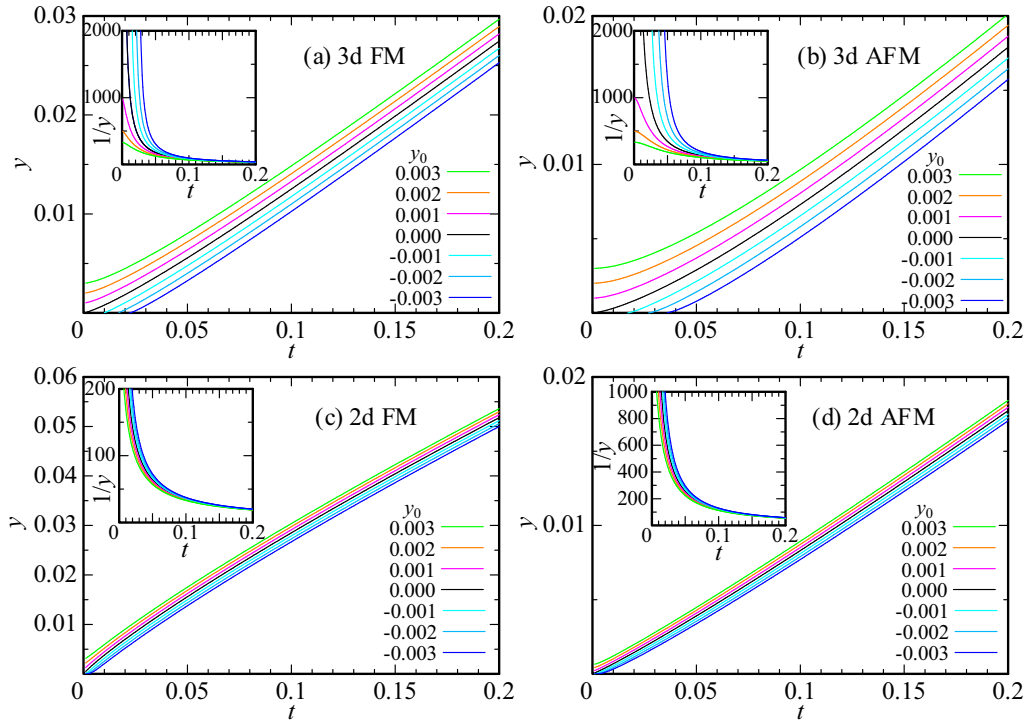


FIG. 1. Scaled temperature dependence of y for (a) 3D FM, (b) 3D AFM, (c), 2D FM, and (d) 2D AFM. The inset shows the scaled temperature dependence of $1/y \propto \chi_Q(0, 0)$.

B. Entropy and specific heat

The entropy $S = -(\frac{\partial \tilde{F}}{\partial T})_V$ is obtained by differentiating the free energy \tilde{F} in Eq. (22) with respect to the temperature. Noting that the terms with $(\frac{\partial \eta}{\partial T})_V$ and also $(\frac{\partial (\varphi^2)_{\text{eff}}}{\partial T})_V$ vanish with the use of the SCR equation [Eq. (16)], the entropy is derived as [27]

$$S = -Nd \int_0^{x_c} dx x^{d-1} \left\{ \ln \sqrt{2\pi} - u + \left(u - \frac{1}{2}\right) \ln u - \ln \Gamma(u) \right\} + Nd \int_0^{x_c} dx x^{d-1} u \left\{ \ln u - \frac{1}{2u} - \psi(u) \right\}, \quad (39)$$

where $\Gamma(u)$ is the Gamma function.

The specific heat under a constant volume is obtained by differentiating the entropy S in Eq. (39) with respect to the

temperature [14,27] as

$$C_V = T \left(\frac{\partial S}{\partial T} \right)_V = C_a - C_b, \quad (40)$$

where C_a and C_b are given by

$$C_a = -Nd \int_0^{x_c} dx x^{d-1} u^2 \left\{ \frac{1}{u} + \frac{1}{2u^2} - \psi'(u) \right\}, \quad (41)$$

$$C_b = \tilde{C}_b \left(\frac{\partial y}{\partial t} \right)_V, \quad (42)$$

respectively. Here $\psi'(u)$ is the trigamma function and \tilde{C}_b is given by

$$\tilde{C}_b = -Nd \int_0^{x_c} dx x^{d+z-3} u \left\{ \frac{1}{u} + \frac{1}{2u^2} - \psi'(u) \right\}. \quad (43)$$

As for C_a , the x integral in Eq. (41) shows no divergence from $x = 0$ even for $y \rightarrow 0$ irrespective of spatial dimensions

TABLE I. Quantum criticality at the magnetic QCP for each class specified by $z = 3$ (FM) and $z = 2$ (AFM) in $d = 3$ and 2 [3]. Electrical resistivity $\rho(T)$, specific-heat coefficient C/T , uniform susceptibility $\chi(T)$, and NMR relaxation rate $(T_1 T)^{-1}$. For χ , \rightarrow C.W. denotes the crossover to the Curie-Weiss behavior. Note that $\eta \propto y$ holds [see Eq. (23)].

Class	η	ρ	C/T	χ	$(T_1 T)^{-1}$	Refs.
3D FM	$T^{4/3}$	$T^{5/3}$	$-\ln T$	$T^{-4/3} \rightarrow$ C.W.	$T^{-4/3}$	[6,12]
3D AFM	$T^{3/2}$	$T^{3/2}$	const. $-T^{1/2}$	const. $-T^{1/4} \rightarrow$ C.W.	$T^{-3/4}$	[11,34]
2D FM	$-T \ln T$	$T^{4/3}$	$T^{-1/3}$	$-1/(T \ln T) \rightarrow$ C.W.	$-1/(T \ln T)^{3/2}$	[10]
2D AFM	$\frac{-T \ln(-\ln T)}{\ln T}$	T	$-\ln T$	-	$-\ln T/T$	[13,35]

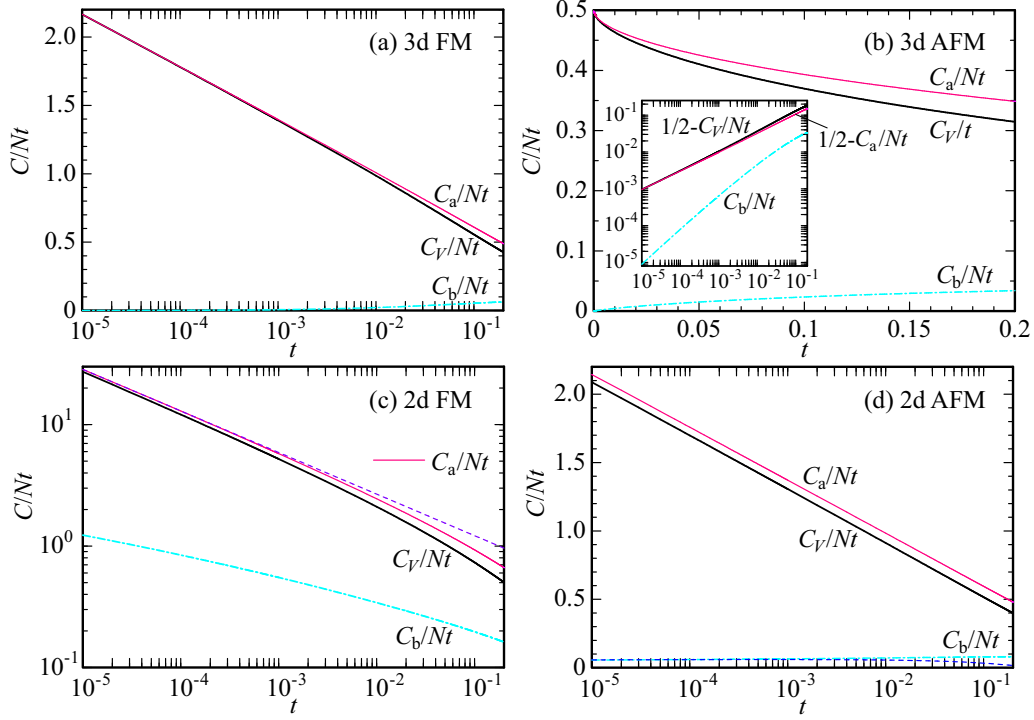


FIG. 2. Specific-heat coefficient vs scaled temperature just at the QCP. C_V/Nt (bold solid line), C_a/Nt (thin line), and C_b/Nt (dash-dotted line) are calculated numerically in Eqs. (40), (41), and (42), respectively for $y_0 = 0.0$ and $y_1 = 1.0$. (a) 3D FM QCP. (b) 3D AFM QCP. The inset shows log-log plot of $1/2 - C_V/Nt$ (thick solid line), $1/2 - C_a/Nt$ (thin solid line), and C_b/Nt (dash-dotted line). (c) 2D FM QCP. The dashed line represents the least-square fit of C_a/Nt for $10^{-5} \leq t \leq 10^{-4}$ with $at^{-1/3}$. (d) 2D AFM QCP. The dashed line represents the least-square fit of C_b/t for $10^{-5} \leq t \leq 10^{-4}$ with $-a \frac{(\ln(-\ln t))^2}{-\ln t}$.

[27]. Hence, C_a for $t \ll 1$ at the QCP has no explicit y dependence.

As for \tilde{C}_b , in $d = 3$, the x integral in Eq. (43) shows no divergence from $x = 0$ for $y \rightarrow 0$ and is evaluated as [27]

$$\frac{\tilde{C}_b}{N} \sim t^{1+\frac{1}{z}}, \quad (44)$$

for $t \rightarrow 0$ at the QCP. Namely, \tilde{C}_b shows the same temperature dependence as y , i.e., $\tilde{C}_b \sim y$, as seen in Eq. (38). In $d = 2$, the x integral in Eq. (43) shows logarithmic divergence arising from $x = 0$ for $y \rightarrow 0$. Hence, \tilde{C}_b has the $\ln y$ dependence at the QCP.

The temperature dependence of the specific heat at the magnetic QCP for each class is summarized in the following subsections. The numerical calculation of Eq. (40) is also performed. To calculate $(\frac{\partial y}{\partial t})_V$, by differentiating the SCR equation [Eqs. (33) and (34)] with respect to the scaled temperature t , we have

$$\left(\frac{\partial y}{\partial t}\right)_V = \begin{cases} \frac{\frac{y_1}{2} \tilde{C}_b \frac{1}{N}}{1 - \frac{dy_1}{2} M} & \text{for } d+z > 4, \\ \frac{\frac{y_1}{2} \tilde{C}_b \frac{1}{N}}{1 - \frac{y_1}{2} (\ln y + 1) - \frac{dy_1}{2} M} & \text{for } d+z = 4, \end{cases} \quad (45)$$

where M is given by

$$M = \int_0^{x_c} dx x^{d+2z-5} \left\{ \frac{1}{u} + \frac{1}{2u^2} - \psi'(u) \right\}. \quad (46)$$

To calculate the t dependence of the specific heat just at the QCP, we set $y_0 = 0.0$ in the SCR equation [Eqs. (33) and (34)]

with setting as $y_1 = 1.0$ and $x_c = 1.0$. By solving the SCR equation, we obtain the solution $y(t)$. Then, by inputting $y(t)$ to Eq. (45), we obtain $(\frac{\partial y}{\partial t})_V$. Finally, by substituting $y(t)$ and $(\frac{\partial y}{\partial t})_V$ into Eq. (40) for each class, we obtain $C_V(t)$, which is shown in Figs. 2(a)–2(d), respectively.

1. 3D ferromagnetic case

For $t \ll 1$, C_a is evaluated as [5,12,27]

$$\frac{C_a}{N} \approx -\frac{t}{6} \ln t. \quad (47)$$

For $t \ll 1$, \tilde{C}_b is evaluated as [27]

$$\frac{\tilde{C}_b}{N} \sim t^{4/3}. \quad (48)$$

Since C_b behaves as $C_b \sim t^{5/3}$ in Eq. (42) with $\partial y/\partial t \sim t^{1/3}$ for $t \ll 1$, the specific heat in Eq. (40) behaves as

$$\frac{C_V}{N} \approx \frac{C_a}{N} \sim -t \ln t, \quad (49)$$

for $t \ll 1$, where the dominant contribution comes from C_a , as seen in Fig. 2(a). This reproduces the criticality shown by the past SCR theory, which is summarized in Table I (see C/T for 3D FM). It is noted that the same temperature dependence as Eq. (49) was also derived from the RG theory [9].

2. 3D antiferromagnetic case

For $t \ll 1$, C_a is evaluated as [11,27]

$$\frac{C_a}{N} \approx \frac{1}{2}t \left(x_c - \frac{15}{2}a_{5/2}^* t^{1/2} \right), \quad (50)$$

where $a_{5/2}^*$ is a constant given by $a_{5/2}^* = \int_0^\infty du u^{3/2} \left\{ \frac{1}{2u^2} - \ln u + \frac{1}{2u} + \psi(u) \right\}$. For $t \ll 1$, \tilde{C}_b is evaluated as [27]

$$\frac{\tilde{C}_b}{N} \sim t^{3/2}. \quad (51)$$

Since C_b behaves as $C_b \sim t^2$ in Eq. (42) with $\partial y / \partial t \sim t^{1/2}$ for $t \ll 1$, the specific heat in Eq. (40) behaves as

$$\frac{C_V}{N} \approx \frac{C_a}{N} \sim \frac{1}{2}t \left(x_c - \frac{15}{2}a_{5/2}^* t^{1/2} \right), \quad (52)$$

for $t \ll 1$, where the dominant contribution comes from C_a , as seen in Fig. 2(b). This reproduces the criticality shown by the past SCR theory (see C/T for 3D AFM in Table I). It is noted that the same temperature dependence as Eq. (52) was also derived from the RG theory [9].

3. 2D ferromagnetic case

For $t \ll 1$, C_a is evaluated as [10,27]

$$\frac{C_a}{N} \approx \frac{10}{9}a_{5/3}t^{2/3}, \quad (53)$$

where a_ν is a constant given by $a_\nu \equiv \pi \zeta(\nu) \Gamma(\nu) / [(2\pi)^\nu \sin(\nu\pi/2)]$ and $a_{5/3} = 0.5629 \dots$. For $y \ll t^{2/3} \ll 1$, we have

$$\frac{\tilde{C}_b}{N} \approx \frac{t}{2} \ln \left[\frac{1}{y} \left(\frac{t}{6} \right)^{2/3} \right]. \quad (54)$$

Since $y \approx -\frac{y_1}{12} t \ln t$ at the QCP is obtained from the SCR equation [Eq. (33)] for $d = 2$ and $z = 3$ by setting $y_0 = 0.0$ [10], we have

$$\frac{\tilde{C}_b}{N} \approx -\frac{t}{6} \ln t. \quad (55)$$

Since the coefficient $\frac{10}{9}a_{5/3}$ in Eq. (53) is the quantity of $O(1)$, which is much larger than that in $\tilde{C}_b \left(\frac{\partial y}{\partial t} \right)_V \sim \frac{y_1}{72} t \ln t (\ln t + 1)$, the specific heat in Eq. (40) is dominated by C_a as

$$\frac{C_V}{N} \approx \frac{C_a}{N} \sim t^{2/3}, \quad (56)$$

for $t \ll 1$. This can be confirmed by numerical calculation of Eq. (40), as shown in Fig. 2(c). This reproduces the criticality shown by the past SCR theory (see C/T for 2D FM in Table I). It is noted that the same temperature dependence as Eq. (56) was also derived from the RG theory [17].

4. 2D antiferromagnetic case

For $t \ll 1$, C_a is evaluated as [27]

$$\frac{C_a}{N} \approx -\frac{t}{6} \ln t. \quad (57)$$

For $y \ll t \ll 1$, \tilde{C}_b is evaluated as

$$\frac{\tilde{C}_b}{N} \approx -\frac{t}{2} \ln \left(6 \frac{y}{t} \right). \quad (58)$$

Since $y \approx -t \frac{\ln(-\ln t)}{2 \ln t}$ at the QCP is obtained from the SCR equation [Eq. (34)] for $d = 2$ and $z = 2$ by setting $y_0 = 0.0$ [35], we have

$$\frac{\tilde{C}_b}{N} \sim t \ln(-\ln t). \quad (59)$$

Since C_b behaves as $C_b \sim -t \frac{(\ln(-\ln t))^2}{\ln t}$ in Eq. (42) with $\partial y / \partial t \sim -\ln(-\ln t) / \ln t$ for $0 < t \ll 1$ [see the dashed line in Fig. 2(c)], the specific heat in Eq. (40) behaves as

$$\frac{C_V}{N} \approx \frac{C_a}{N} \sim -t \ln t, \quad (60)$$

for $t \ll 1$, where the dominant contribution comes from C_a , as seen in Fig. 2(d). This reproduces the criticality shown by the past SCR theory (see C/T for 2D AFM in Table I). It is noted that the same temperature dependence as Eq. (60) was also derived from the RG theory [17].

IV. GRÜNEISEN PARAMETER NEAR THE MAGNETIC QCP

The Grüneisen parameter Γ near the magnetic QCP is derived on the basis of Eq. (8) in the SCR theory. The calculation starts from the entropy S in Eq. (39). By differentiating both sides of Eq. (39) with respect to the volume V under a constant entropy S , we have

$$0 = Nd \int_0^{x_c} dx x^{d-1} \left(\frac{\partial u}{\partial V} \right)_S u \left\{ \frac{1}{u} + \frac{1}{2u^2} - \psi'(u) \right\}, \quad (61)$$

where $(\partial u / \partial V)_S$ is given by

$$\left(\frac{\partial u}{\partial V} \right)_S = \frac{1}{t} \left\{ x^{z-2} \left(\frac{\partial y}{\partial V} \right)_S - u \left(\frac{\partial t}{\partial V} \right)_S \right\}. \quad (62)$$

Then, substituting Eq. (62) into Eq. (61) we have

$$\left(\frac{\partial t}{\partial V} \right)_S = \frac{\tilde{C}_b \left(\frac{\partial y}{\partial V} \right)_S}{C_a}, \quad (63)$$

where C_a and \tilde{C}_b are defined by Eqs. (41) and (43), respectively. By differentiating Eq. (32) with respect to the volume V under a constant entropy S , we have

$$\left(\frac{\partial t}{\partial V} \right)_S = \frac{1}{T_0} \left(\frac{\partial T}{\partial V} \right)_S - \frac{T}{T_0^2} \left(\frac{\partial T_0}{\partial V} \right)_S. \quad (64)$$

By substituting Eq. (64) into Eq. (63), the Grüneisen parameter [Eq. (8)] is expressed as follows:

$$\Gamma = -\frac{\tilde{C}_b}{C_a} \frac{V}{t} \left(\frac{\partial y}{\partial V} \right)_S - \frac{V}{T_0} \left(\frac{\partial T_0}{\partial V} \right)_S. \quad (65)$$

This is one of the central results of the present paper, whose property will be discussed in detail in Sec. VII. The second term expresses the volume derivative of the characteristic temperature of spin fluctuation. The first term is proportional to \tilde{C}_b , which gives a minor contribution to C_V as shown in Fig. 2. However, this term gives the dominant contribution to Γ at low temperatures, which will be shown in Sec. VII.

The Grüneisen parameter Γ can also be derived from Eq. (6) with the specific heat C_V in Eq. (40) and the thermal-expansion coefficient α defined by Eq. (3) or by Eq. (5). Each

derivation will be shown in the following Secs. **VC** and **VA**, respectively.

V. THERMAL-EXPANSION COEFFICIENT NEAR THE MAGNETIC QCP

So far, in the theory of spin fluctuations, the thermal-expansion coefficient α in itinerant magnets has been discussed on the basis of Eq. (3) [27]. In Sec. **VA** we will show that α can be derived from Eq. (5) in a much simpler form in the SCR theory, which enables us to capture the physical picture. Next, we will derive α by the standard way from Eq. (3) in Secs. **VB** and **VC**. It will be shown that the result is lengthy, where it is hard to see an immediate correspondence to the result obtained in Sec. **VA**, although both should be equivalent from the viewpoint of the thermodynamic relation as shown in Sec. **II**. To show the equivalence in the SCR theory explicitly, the proof will be given in Sec. **VD**.

A. Derivation from $\alpha = -\frac{1}{V}(\frac{\partial S}{\partial P})_T$

First, let us derive the thermal-expansion coefficient α defined by Eq. (5). Then, calculation starts from the entropy

S in Eq. (39). By differentiating the entropy S with respect to the pressure P under a constant temperature, we obtain

$$\left(\frac{\partial S}{\partial P}\right)_T = -\frac{\tilde{C}_b}{t}\left(\frac{\partial y}{\partial P}\right)_T - \frac{C_a}{T_0}\left(\frac{\partial T_0}{\partial P}\right)_T, \quad (66)$$

where \tilde{C}_b and C_a appeared in the formula of the specific heat, which are given by Eqs. (43) and (41), respectively. Then, the thermal-expansion coefficient is obtained as

$$\alpha = -\frac{1}{V}\left(\frac{\partial S}{\partial P}\right)_T \quad (67)$$

$$= \alpha_a + \alpha_b, \quad (68)$$

where α_a and α_b are defined by

$$\alpha_a \equiv \frac{1}{V}\frac{C_a}{T_0}\left(\frac{\partial T_0}{\partial P}\right)_T, \quad (69)$$

$$\alpha_b \equiv \frac{1}{V}\frac{\tilde{C}_b}{t}\left(\frac{\partial y}{\partial P}\right)_T, \quad (70)$$

respectively. This is one of the central results of the present paper, whose property will be discussed in detail in Sec. **VI**.

B. Pressure near the magnetic QCP

Next, let us derive the pressure $P = -(\frac{\partial \tilde{F}}{\partial V})_T$ starting from the free energy in Eq. (22). By differentiating Γ_q [Eq. (24)] with respect to the volume V under a constant temperature, we have

$$\left(\frac{\partial \Gamma_q}{\partial V}\right)_T = 2\pi\left(\frac{\partial T_0}{\partial V}\right)_T x^{z-2}(y+x^2) + 2\pi T_0 x^{z-2}\left(\frac{\partial y}{\partial V}\right)_T. \quad (71)$$

In the calculation of $(\frac{\partial \tilde{F}}{\partial V})_T$, the terms with $(\frac{\partial y}{\partial V})_T$ and also $(\frac{\partial \langle \varphi^2 \rangle_{\text{eff}}}{\partial V})_T$ vanish because of the SCR equation [Eq. (16)] or optimization condition $d\tilde{F}(y)/dy = 0$ [28]. The details are given in Appendix **E**. Then, only the first term with $(\frac{\partial T_0}{\partial V})_T$ in Eq. (71) remains and we have

$$P = -\left(\frac{\partial \tilde{F}}{\partial V}\right)_T = -\frac{1}{T_0}\left(\frac{\partial T_0}{\partial V}\right)_T I - \left[\frac{\partial}{\partial V}\left(\frac{\eta_0}{Aq_B^2}\right)\right]_T T_A \langle \varphi^2 \rangle_{\text{eff}} - \left(\frac{\eta_0}{Aq_B^2} - y\right)\left(\frac{\partial T_A}{\partial V}\right)_T \langle \varphi^2 \rangle_{\text{eff}} - \frac{3}{N}\left(\frac{\partial v_4}{\partial V}\right)_T \langle \varphi^2 \rangle_{\text{eff}}^2, \quad (72)$$

where I is given by

$$I = \frac{1}{\pi} \sum_q \int_0^{\omega_c} d\omega \Gamma_q \frac{\partial}{\partial \Gamma_q} \left(\frac{\Gamma_q}{\omega^2 + \Gamma_q^2} \right) \left[\frac{\omega}{2} + T \ln(1 - e^{-\frac{\omega}{T}}) \right]. \quad (73)$$

Here, by using the relation [27]

$$\frac{\partial}{\partial \Gamma_q} \left(\frac{\Gamma_q}{\omega^2 + \Gamma_q^2} \right) = -\frac{\partial}{\partial \omega} \left(\frac{\omega}{\omega^2 + \Gamma_q^2} \right), \quad (74)$$

the partial integration with respect to ω can be performed. Then we have

$$I = \frac{1}{\pi} \sum_q \Gamma_q \left\{ -\frac{\omega}{\omega^2 + \Gamma_q^2} \left[\frac{\omega}{2} + T \ln(1 - e^{-\frac{\omega}{T}}) \right] \right\} \Big|_0^{\omega_c} + \int_0^{\omega_c} d\omega \frac{\omega}{\omega^2 + \Gamma_q^2} \left(\frac{1}{2} + \frac{1}{e^{\frac{\omega}{T}} - 1} \right). \quad (75)$$

The first line in Eq. (75) is neglected since the spectrum of the spin fluctuation is considered to decrease faster than the Lorentzian in the high-frequency regime [27]. Hence, the first and second terms in the last line in Eq. (75) are expressed as

$$I = I_{\text{zero}} + I_{\text{th}}, \quad (76)$$

respectively, where I_{zero} is given by

$$I_{\text{zero}} = \frac{NdT_0t}{2} \int_0^{\omega_c} dx x^{d-1} u \ln \left| \frac{\omega_{cT}^2 + u^2}{u^2} \right|, \quad (77)$$

and I_{th} is given by

$$I_{\text{th}} = NdT_0t \int_0^{x_c} dx x^{d-1} u \left\{ \ln u - \frac{1}{2u} - \psi(u) \right\}. \quad (78)$$

C. Derivation from $\alpha = \kappa_T \left(\frac{\partial P}{\partial T} \right)_V$

Let us derive the thermal-expansion coefficient α defined by $\alpha \equiv \kappa_T \left(\frac{\partial P}{\partial T} \right)_V$ in Eq. (3), where the isothermal compressibility is given by Eq. (4). By differentiating the pressure in Eq. (72) with respect to the temperature T under a constant volume V , we have

$$\begin{aligned} \frac{\alpha}{\kappa_T} = \left(\frac{\partial P}{\partial T} \right)_V = & -\frac{1}{T_0} \left(\frac{\partial T_0}{\partial V} \right)_T \left[\left(\frac{\partial I_{\text{zero}}}{\partial T} \right)_V + \left(\frac{\partial I_{\text{th}}}{\partial T} \right)_V \right] - \frac{\partial}{\partial T} \left[\left[\frac{\partial}{\partial V} \left(\frac{\eta_0}{Aq_B^2} \right) \right]_T T_A \langle \varphi^2 \rangle_{\text{eff}} \right. \\ & \left. + \left(\frac{\eta_0}{Aq_B^2} - y \right) \left(\frac{\partial T_A}{\partial V} \right)_T \langle \varphi^2 \rangle_{\text{eff}} + \frac{3}{N} \left(\frac{\partial v_4}{\partial V} \right)_T \langle \varphi^2 \rangle_{\text{eff}}^2 \right] \Big|_V, \end{aligned} \quad (79)$$

where

$$\left(\frac{\partial I_{\text{zero}}}{\partial T} \right)_V = Nd \left(\frac{\partial y}{\partial t} \right)_V \left\{ \frac{1}{2} \int_0^{x_c} dx x^{d+z-3} \ln \left| \frac{\omega_{cT}^2 + u^2}{u^2} \right| - \int_0^{x_c} dx x^{d+z-3} \frac{\omega_{cT}^2}{\omega_{cT}^2 + u^2} \right\}, \quad (80)$$

$$\left(\frac{\partial I_{\text{th}}}{\partial T} \right)_V = \left(\frac{\partial y}{\partial t} \right)_V (NdL - \tilde{C}_b) + C_a. \quad (81)$$

Here L is given by

$$L = \int_0^{x_c} dx x^{d+z-3} \left\{ \ln u - \frac{1}{2u} - \psi(u) \right\}. \quad (82)$$

By substituting Eqs. (80) and (81) into Eq. (79), we obtain

$$\begin{aligned} \frac{\alpha}{\kappa_T} = & \frac{1}{T_0} \left(\frac{\partial T_0}{\partial V} \right)_T \left[\left(\frac{\partial y}{\partial t} \right)_V \left\{ -\frac{Nd}{2} \int_0^{x_c} dx x^{d+z-3} \ln \left| \frac{\omega_{cT}^2 + u^2}{u^2} \right| + Nd \int_0^{x_c} dx x^{d+z-3} \frac{\omega_{cT}^2}{\omega_{cT}^2 + u^2} - NdL + \tilde{C}_b \right\} - C_a \right] \\ & - \left(\frac{\partial y}{\partial t} \right)_V \left\{ \frac{N}{6v_4} \frac{T_A^2}{T_0} \left[\frac{\partial}{\partial V} \left(\frac{\eta_0}{Aq_B^2} \right) \right]_T - \frac{2}{T_0} \langle \varphi^2 \rangle_{\text{eff}} \left(\frac{\partial T_A}{\partial V} \right)_T + \frac{T_A}{T_0} \langle \varphi^2 \rangle_{\text{eff}} \frac{1}{v_4} \left(\frac{\partial v_4}{\partial V} \right)_T \right\}, \end{aligned} \quad (83)$$

where the last three terms have been obtained by using the SCR equation [Eq. (16)]. Details are given in Appendix F.

D. Equivalence of the expressions of thermal-expansion coefficients

In Secs. VA and VC, each expression of the thermal-expansion coefficient α has been derived from Eqs. (5) and (3), respectively. At first glance, it seems unclear whether Eqs. (68) and (83) are equivalent. However, with the use of the stationary condition of the SCR theory, it can be shown that both expressions are equivalent, which will be proven in this subsection.

Multiplying κ_T on both sides of Eq. (83) and using Eq. (4) with the relation $\left(\frac{\partial V}{\partial P} \right)_T \left(\frac{\partial Y}{\partial V} \right)_T = \left(\frac{\partial Y}{\partial P} \right)_T$ for $Y = T_0, \eta_0, N_F,$ and v_4 , we obtain

$$\begin{aligned} \alpha = & \frac{1}{V} \frac{1}{T_0} \left(\frac{\partial T_0}{\partial P} \right)_T \left[C_a + \left(\frac{\partial y}{\partial t} \right)_V \left\{ NdL - \tilde{C}_b + \frac{Nd}{2} \int_0^{x_c} dx x^{d+z-3} \ln \left| \frac{\omega_{cT}^2 + u^2}{u^2} \right| - Nd \int_0^{x_c} dx x^{d+z-3} \frac{\omega_{cT}^2}{\omega_{cT}^2 + u^2} \right\} \right] \\ & + \frac{1}{V} \left(\frac{\partial y}{\partial t} \right)_V \left\{ \frac{N}{6v_4} \frac{T_A^2}{T_0} \left[\frac{\partial}{\partial P} \left(\frac{\eta_0}{Aq_B^2} \right) \right]_T - \frac{2}{T_0} \langle \varphi^2 \rangle_{\text{eff}} \left(\frac{\partial T_A}{\partial P} \right)_T + \frac{T_A}{T_0} \langle \varphi^2 \rangle_{\text{eff}} \frac{1}{v_4} \left(\frac{\partial v_4}{\partial P} \right)_T \right\}. \end{aligned} \quad (84)$$

Near the QCP, the x integration on the first line of Eq. (84) is expanded around $y = 0$ as

$$\int_0^{x_c} dx x^{d+z-3} \ln \left| \frac{\omega_{cT}^2 + u^2}{u^2} \right| = \begin{cases} C_1 - C_2 y + \dots & (d+z > 4), \\ C_1 + y \ln y - C_2 y + \dots & (d+z = 4), \end{cases} \quad (85)$$

where C_1 and C_2 are given by Eqs. (28) and (29), respectively. On the last term in the first line of Eq. (84), the x integration is also expanded around $y = 0$ and we obtain

$$-\frac{1}{T_0} \left(\frac{\partial T_0}{\partial P} \right)_T \int_0^{x_c} dx x^{d+z-3} \frac{\omega_{cT}^2}{\omega_{cT}^2 + u^2} = \frac{1}{2} \left\{ \left(\frac{\partial C_1}{\partial P} \right)_T - \left(\frac{\partial C_2}{\partial P} \right)_T y \right\} + \dots, \quad (86)$$

whose derivation is given in Appendix G.

By substituting the SCR equation [Eq. (33)] into y which appears on the r.h.s. of Eqs. (85) and (86), and $\langle \varphi^2 \rangle_{\text{eff}}$ in the last line of Eq. (84), Eq. (84) is expressed as

$$\alpha = \frac{1}{V} \frac{1}{T_0} \left(\frac{\partial T_0}{\partial P} \right)_T C_a + \frac{1}{V} \left(\frac{\partial y}{\partial t} \right)_V \left[-\frac{1}{T_0} \left(\frac{\partial T_0}{\partial P} \right)_T \tilde{C}_b + N \frac{2}{y_1} \left\{ \left(\frac{\partial y_0}{\partial P} \right)_T + \left(\frac{\partial y_1}{\partial P} \right)_T \frac{d}{2} L \right\} \right], \quad (87)$$

for $d + z > 4$. The details of the derivation are given in Appendix H. Here the following equations, which are obtained by differentiating Eqs. (35) and (36) with respect to the pressure, respectively, are used to derive the second line of Eq. (87):

$$\begin{aligned} \left(\frac{\partial y_0}{\partial P} \right)_T &= \left\{ \frac{1}{T_0} \left(\frac{\partial T_0}{\partial P} \right)_T - \frac{2}{T_A} \left(\frac{\partial T_A}{\partial P} \right)_T + \frac{1}{v_4} \left(\frac{\partial v_4}{\partial P} \right)_T \right\} \frac{d}{4} y_1 (C_1 - C_2 y_0) \\ &\quad + \frac{d}{4} y_1 \left\{ \left(\frac{\partial C_1}{\partial P} \right)_T - \left(\frac{\partial C_2}{\partial P} \right)_T y_0 \right\} + \left[\frac{\partial}{\partial P} \left(\frac{\eta_0}{Aq_B^2} \right) \right]_T \frac{1}{Aq_B^2} \frac{y_1}{12v_4 \frac{T_0}{T_A^2}}, \end{aligned} \quad (88)$$

$$\left(\frac{\partial y_1}{\partial P} \right)_T = \left\{ \frac{1}{T_0} \left(\frac{\partial T_0}{\partial P} \right)_T - \frac{2}{T_A} \left(\frac{\partial T_A}{\partial P} \right)_T + \frac{1}{v_4} \left(\frac{\partial v_4}{\partial P} \right)_T \right\} y_1 \left(1 - \frac{d}{4} C_2 y_1 \right) - \frac{d}{4} y_1^2 \left(\frac{\partial C_2}{\partial P} \right)_T. \quad (89)$$

For $d + z = 4$, by substituting the SCR equation [Eq. (34)] into Eq. (86) and with the use of Eqs. (88) and (89), Eq. (84) is shown to lead to

$$\alpha = \frac{1}{V} \frac{1}{T_0} \left(\frac{\partial T_0}{\partial P} \right)_T C_a + \frac{1}{V} \left(\frac{\partial y}{\partial t} \right)_V \left[-\frac{1}{T_0} \left(\frac{\partial T_0}{\partial P} \right)_T \tilde{C}_b + N \frac{2}{y_1} \left\{ \left(\frac{\partial y_0}{\partial P} \right)_T + \left(\frac{\partial y_1}{\partial P} \right)_T \left(L + \frac{1}{2} y \ln y \right) \right\} \right], \quad (90)$$

which has a form with a logarithmic term in the last term in Eq. (87).

The results of Eqs. (87) and (90) are consequences of the fact that the quantities T_0 , T_A , v_4 , and $\eta_0/(Aq_B^2)$, which are included in y_0 and/or y_1 defined by Eqs. (35) and (36), respectively, have the pressure dependence. Since T_0 is included in the constants C_1 and C_2 , as seen in Eqs. (28) and (29), respectively, the pressure dependencies appear via T_0 .

By substituting Eq. (45) into Eqs. (87) and (90), the thermal-expansion coefficient is expressed as

$$\alpha = \alpha_a + \alpha_b, \quad (91)$$

where α_a is given by

$$\alpha_a = \frac{1}{V} \frac{1}{T_0} \left(\frac{\partial T_0}{\partial P} \right)_T C_a, \quad (92)$$

and α_b is given by

$$\alpha_b = \frac{1}{V} \frac{\tilde{C}_b \left[\left(\frac{\partial y_0}{\partial P} \right)_T + \left(\frac{\partial y_1}{\partial P} \right)_T \frac{d}{2} L - \frac{1}{T_0} \left(\frac{\partial T_0}{\partial P} \right)_T \tilde{C}_b \frac{y_1}{2} \frac{1}{N} \right]}{1 - \frac{dy_1}{2t} M}, \quad (93)$$

for $d + z > 4$, and

$$\alpha_b = \frac{1}{V} \frac{\tilde{C}_b \left[\left(\frac{\partial y_0}{\partial P} \right)_T + \left(\frac{\partial y_1}{\partial P} \right)_T \left(\frac{d}{2} L + \frac{1}{2} y \ln y \right) - \frac{1}{T_0} \left(\frac{\partial T_0}{\partial P} \right)_T \tilde{C}_b \frac{y_1}{2} \frac{1}{N} \right]}{1 - \frac{y_1}{2} (\ln y + 1) - \frac{dy_1}{2t} M}, \quad (94)$$

for $d + z = 4$, respectively.

On the other hand, let us turn to Eq. (68) to be compared with Eqs. (91) and (94). We see that Eq. (69) is exactly the same as Eq. (92). As for α_b , to calculate $\left(\frac{\partial y}{\partial P} \right)_T$, by differentiating the SCR equation [Eq. (33) and Eq. (34)] with respect to the pressure P , we obtain

$$\left(\frac{\partial y}{\partial P} \right)_T = \begin{cases} \frac{\left(\frac{\partial y_0}{\partial P} \right)_T + \left(\frac{\partial y_1}{\partial P} \right)_T \frac{d}{2} L - \frac{1}{T_0} \left(\frac{\partial T_0}{\partial P} \right)_T \tilde{C}_b \frac{y_1}{2} \frac{1}{N}}{1 - \frac{dy_1}{2t} M} & (d + z > 4), \\ \frac{\left(\frac{\partial y_0}{\partial P} \right)_T + \left(\frac{\partial y_1}{\partial P} \right)_T \left(\frac{d}{2} L + \frac{1}{2} y \ln y \right) - \frac{1}{T_0} \left(\frac{\partial T_0}{\partial P} \right)_T \tilde{C}_b \frac{y_1}{2} \frac{1}{N}}{1 - \frac{y_1}{2} (\ln y + 1) - \frac{dy_1}{2t} M} & (d + z = 4), \end{cases} \quad (95)$$

respectively. By substituting Eq. (95) into Eq. (70), α_b is obtained as

$$\alpha_b = \frac{1}{V} \frac{\tilde{C}_b \left[\left(\frac{\partial y_0}{\partial P} \right)_T + \left(\frac{\partial y_1}{\partial P} \right)_T \frac{d}{2} L - \frac{1}{T_0} \left(\frac{\partial T_0}{\partial P} \right)_T \tilde{C}_b \frac{y_1}{2} \frac{1}{N} \right]}{1 - \frac{dy_1}{2t} M}, \quad (96)$$

for $d + z > 4$, and

$$\alpha_b = \frac{1}{V} \frac{\tilde{C}_b \left[\left(\frac{\partial y_0}{\partial P} \right)_T + \left(\frac{\partial y_1}{\partial P} \right)_T \left(\frac{d}{2} L + \frac{1}{2} y \ln y \right) - \frac{1}{T_0} \left(\frac{\partial T_0}{\partial P} \right)_T \tilde{C}_b \frac{y_1}{2} \frac{1}{N} \right]}{1 - \frac{y_1}{2} (\ln y + 1) - \frac{dy_1}{2t} M}, \quad (97)$$

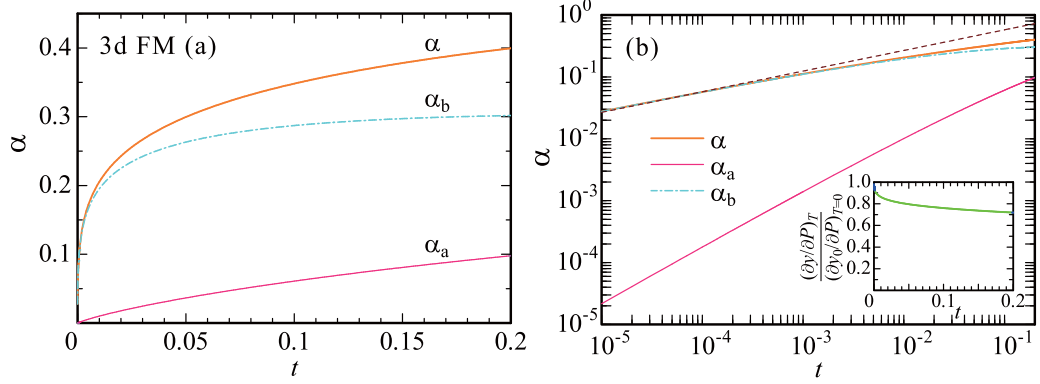


FIG. 3. (a) Temperature dependence of the thermal-expansion coefficient α (thick solid line), α_a (thin solid line), and α_b (dash-dotted line) at the 3D FM QCP. (b) Log-log plot of (a). The dashed line represents the least-square fit of α with $t^{1/3}$ for $10^{-5} \leq t \leq 10^{-4}$. The inset shows the t dependence of $(\frac{\partial^2 y}{\partial P^2})_T / (\frac{\partial^2 y}{\partial P^2})_{T=0}$.

for $d+z=4$, respectively. Now we see that Eq. (96) is exactly the same as Eq. (93) for $d+z>4$. We also see that Eq. (97) is exactly the same as Eq. (94) for $d+z=4$. Hence, it is proven that both expressions on α of Eqs. (68) and (83) are equivalent.

VI. NUMERICAL RESULTS ON THERMAL-EXPANSION COEFFICIENT α AT THE MAGNETIC QCP

Since equivalence of Eqs. (68) and (83) has been proven, let us analyze the temperature dependence of the thermal-expansion coefficient α on the basis of Eq. (68), which has a simpler expression. In Eq. (68), α_b [Eq. (70)] includes $(\frac{\partial y}{\partial P})_T$, which can be obtained by calculating the r.h.s. of Eq. (95). Namely, when the pressure derivatives of T_0 , T_A , v_4 , and $\eta_0/(Aq_B^2)$ are given, one can obtain $(\frac{\partial y_0}{\partial P})_T$ by Eq. (88) and $(\frac{\partial y_1}{\partial P})_T$ by Eq. (89). Then, substituting them into Eq. (95), one obtains the temperature dependence of $(\frac{\partial y}{\partial P})_T$. At the QCP tuned to the critical pressure $P = P_c$, $y_0 = 0$ is realized. However, $(\frac{\partial y_0}{\partial P})_{T=0}$ can have a nonzero value at the QCP in general, which will be shown for $d+z>4$ below. Since y_0 defined by Eq. (35) is the quantity for $T=0$, the first terms in the numerator and denominator of the r.h.s. of Eq. (95) are constants. Note that y_1 defined by Eq. (36) is the quantity for $T=0$ and hence $(\frac{\partial y_1}{\partial P})_T$ has no temperature dependence. Since T_0 is defined by Eq. (25), $(\frac{\partial T_0}{\partial P})_T$ also has no temperature dependence.

To see the temperature dependence of α at the QCP, numerical calculation of Eq. (68) is performed. First, we solve the SCR equation [Eq. (33) or (34)] by setting $y_0 = 0.0$ and $y_1 = 1.0$. With the use of the solution y and $(\frac{\partial y}{\partial T})_V$ obtained by Eq. (45), we calculate $C_a(t)$ in Eq. (41) and $\tilde{C}_b(t)$ in Eq. (43). Then we calculate $(\frac{\partial y}{\partial P})_T$ in Eq. (95) by setting $(\frac{\partial y_0}{\partial P})_T = 1.0$, $(\frac{\partial y_1}{\partial P})_T = 1.0$, and $\frac{1}{T_0}(\frac{\partial T_0}{\partial P})_T = 1.0$ as representative values (the reason for this parametrization is explained below). Finally, by substituting $C_a(t)$, $\tilde{C}_b(t)$, and $(\frac{\partial y}{\partial P})_T$ into Eq. (68), we obtain the temperature dependence of $\alpha(t)$ at the QCP. In the plot of $\alpha(t)$, the lattice constant is set as unity. The results for each universality class are shown in Figs. 3,

4, 5, and 6, respectively, whose properties are analyzed in the following subsections.

Before going into a detailed analysis of $\alpha(t)$, here we comment on the unit and parametrization. In Eq. (68), the volume V is regarded as the molar volume. Then, by multiplying the value of $\frac{1}{T_0}(\frac{\partial T_0}{\partial P})_T$ in the unit of GPa^{-1} to the restored Boltzmann constant over the unit-cell volume k_B/V_{unit} , where V_{unit} is given by $V_{\text{unit}} = a[\text{\AA}] \times b[\text{\AA}] \times c[\text{\AA}]$, we obtain α_a in the unit of K^{-1} , as follows:

$$\alpha_a = \frac{1.38}{abc} \times 10^{-2} \times \frac{1}{T_0} \left(\frac{\partial T_0}{\partial P} \right)_T \times \frac{C_a}{N} \quad [\text{K}^{-1}]. \quad (98)$$

As for α_b , by multiplying the value of $(\frac{\partial y}{\partial P})_T$ in the unit of GPa^{-1} to k_B/V_{unit} , we obtain α_b in the unit of K^{-1} , as follows:

$$\alpha_b = \frac{1.38}{abc} \times 10^{-2} \times \left(\frac{\partial y}{\partial P} \right)_T \times \frac{\tilde{C}_b}{Nt} \quad [\text{K}^{-1}]. \quad (99)$$

Hence, multiplying the numerical value of the underlined part of Eqs. (98) and (99) for each material to α_a and α_b , respectively, in the following Figs. 3–6, direct comparison with experiments can be made. More detailed discussion about experiments will be given in Sec. IX C 1.

A. 3D ferromagnetic case

Figure 3(a) shows the temperature dependence of the thermal-expansion coefficient α at the FM QCP ($z=3$) in $d=3$. As t decreases, α_b in Eq. (68) contributes to α dominantly, $\alpha \approx \frac{1}{V} \frac{\tilde{C}_b}{t} (\frac{\partial y}{\partial P})_T$, while contribution from α_a becomes not negligible as t increases.

For $t \ll 1$, we estimate $L \sim t^{4/3}$, $\tilde{C}_b \sim t^{4/3}$, and $M \sim -t^{4/3}$ in Eq. (95). Hence, we have $(\frac{\partial y}{\partial P})_T \approx (\frac{\partial y_0}{\partial P})_{T=0} - b_1 t^{1/3}$ with b_1 being a positive constant. This can be seen in the inset of Fig. 3(b) where the t dependence of $(\frac{\partial y}{\partial P})_T / (\frac{\partial y_0}{\partial P})_{T=0}$ is plotted. At sufficiently low temperatures where $(\frac{\partial y}{\partial P})_T$ can be regarded as a constant $(\frac{\partial y}{\partial P})_T \approx (\frac{\partial y_0}{\partial P})_{T=0}$, α behaves as

$$\alpha \propto \frac{\tilde{C}_b}{t} \sim t^{1/3}, \quad (100)$$

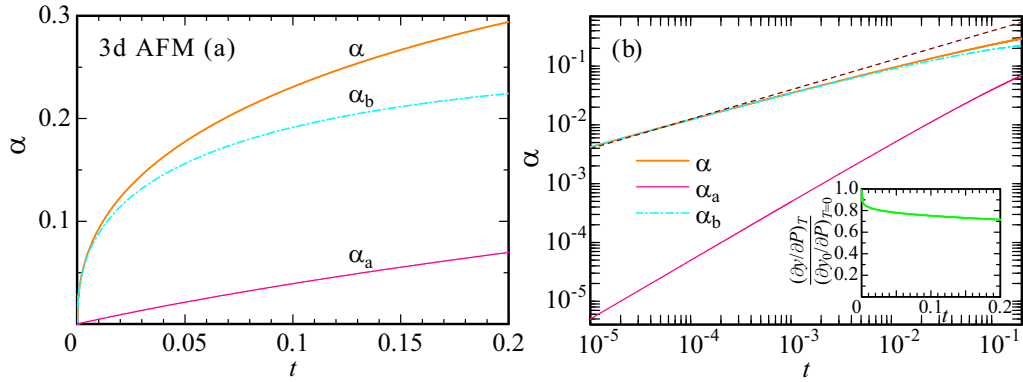


FIG. 4. (a) Temperature dependence of the thermal-expansion coefficient α (thick solid line), α_a (thin solid line), and α_b (dash-dotted line) at the 3D AFM QCP. (b) Log-log plot of (a). The dashed line represents the least-square fit of α with $at^{1/2}$ for $10^{-5} \leq t \leq 10^{-4}$. The inset shows the t dependence of $(\frac{\partial^2 y}{\partial P^2})_T / (\frac{\partial^2 y_0}{\partial P^2})_{T=0}$.

where $\frac{\tilde{C}_b}{t} \sim t^{1/3}$ dominates over $C_a \sim -t \ln t$ [Eq. (49)] in Eq. (68). This coincides with the temperature dependence of the critical part shown by the RG theory [17]. However, it should be noted that $\alpha \sim t^{1/3}$ appears at sufficiently low temperatures for $t \lesssim 10^{-3}$, as shown in Fig. 3(b). This is because the temperature dependent $(\frac{\partial y}{\partial P})_T$ exists in α_b in Eq. (70), as noted above.

B. 3D antiferromagnetic case

Figure 4(a) shows the temperature dependence of the thermal-expansion coefficient α at the AFM QCP ($z = 2$) in $d = 3$. As t decreases, α_b in Eq. (68) contributes to α dominantly, $\alpha \approx \frac{1}{V} \frac{\tilde{C}_b}{t} (\frac{\partial y}{\partial P})_T$, while contribution from α_a becomes not negligible as t increases.

For $t \ll 1$, we estimate $L \sim t^{3/2}$, $\tilde{C}_b \sim t^{3/2}$, and $M \sim -t^{5/4}$ in Eq. (95). Hence, we have $(\frac{\partial y}{\partial P})_T \approx (\frac{\partial y_0}{\partial P})_{T=0} - b_2 t^{1/4}$ with b_2 being a positive constant. This can be seen in the inset of Fig. 4(b) where the t dependence of $(\frac{\partial y}{\partial P})_T / (\frac{\partial y_0}{\partial P})_{T=0}$ is plotted. At sufficiently low temperatures where $(\frac{\partial y}{\partial P})_T$ can

be regarded as a constant $(\frac{\partial y}{\partial P})_T \approx (\frac{\partial y_0}{\partial P})_{T=0}$, α behaves as

$$\alpha \propto \frac{\tilde{C}_b}{t} \sim t^{1/2}, \quad (101)$$

where $\frac{\tilde{C}_b}{t} \sim t^{1/2}$ dominates over $C_a \sim t(\text{const.} - t^{1/2})$ [Eq. (52)] in Eq. (68). This coincides with the temperature dependence of the critical part shown by the RG theory [17]. It should be noted however that $\alpha \sim t^{1/2}$ appears at sufficiently low temperatures for $t \lesssim 10^{-3}$, as shown in Fig. 4(b). This is due to the temperature dependence of $(\frac{\partial y}{\partial P})_T$ in α_b in Eq. (70), as noted above.

C. 2D ferromagnetic case

Figure 5(a) shows the temperature dependence of the thermal-expansion coefficient α at the FM QCP ($z = 3$) in $d = 2$. As t decreases, α_b in Eq. (68) contributes to α dominantly, $\alpha \approx \frac{1}{V} \frac{\tilde{C}_b}{t} (\frac{\partial y}{\partial P})_T$, while contribution from α_a becomes not negligible as t increases.

For $t \ll 1$, we estimate $L \sim -t \ln t$, $\tilde{C}_b \sim -t \ln t$, and $M \sim t / \ln t$ in Eq. (95). Hence, we have $(\frac{\partial y}{\partial P})_T \approx (\frac{\partial y_0}{\partial P})_{T=0} +$

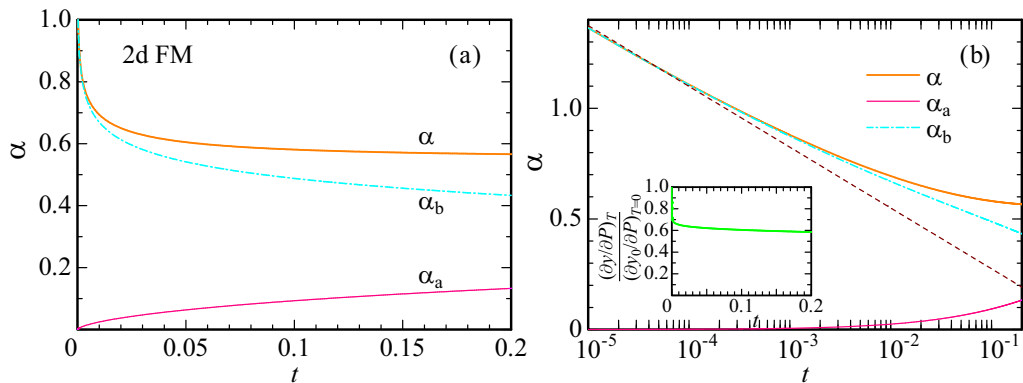


FIG. 5. (a) Temperature dependence of the thermal-expansion coefficient α (thick solid line), α_a (thin solid line), and α_b (dash-dotted line) at the 2D FM QCP. (b) Semi-log plot of (a). The dashed line represents the least-square fit of α with $a \ln t$ for $10^{-5} \leq t \leq 10^{-4}$. The inset shows the t dependence of $(\frac{\partial^2 y}{\partial P^2})_T / (\frac{\partial^2 y_0}{\partial P^2})_{T=0}$.

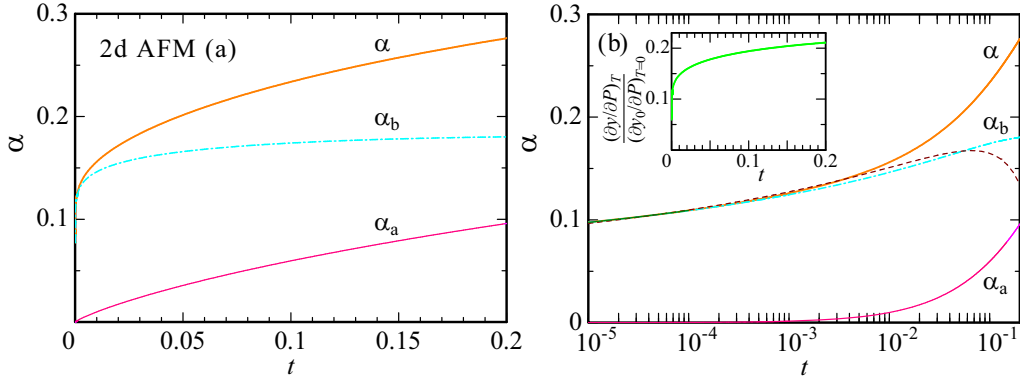


FIG. 6. (a) Temperature dependence of the thermal-expansion coefficient α (thick solid line), α_a (thin solid line), and α_b (dash-dotted line) at the 2D AFM QCP. (b) Semi-log plot of (a). The dashed line represents the least-square fit of α with $-a \frac{\ln(-\ln t)}{\ln t}$ for $10^{-7} \leq t \leq 10^{-4}$. The inset shows the t dependence of $(\frac{\partial y}{\partial P})_T / (\frac{\partial y_0}{\partial P})_{T=0}$.

$b_{3a}/\ln t + b_{3b}t^{1/3}$ with b_{3a} and b_{3b} being positive constants. This can be seen in the inset of Fig. 5(b), where the t dependence of $(\frac{\partial y}{\partial P})_T / (\frac{\partial y_0}{\partial P})_{T=0}$ is plotted. At sufficiently low temperatures where $(\frac{\partial y}{\partial P})_T$ can be regarded as a constant $(\frac{\partial y}{\partial P})_T \approx (\frac{\partial y_0}{\partial P})_{T=0}$, α behaves as

$$\alpha \propto \frac{\tilde{C}_b}{t} \sim -\ln t, \quad (102)$$

where $\frac{\tilde{C}_b}{t} \sim -\ln t$ dominates over $C_a \sim t^{2/3}$ [Eq. (56)] in Eq. (68). This coincides with the temperature dependence of the critical part shown by the RG theory [17]. It should be noted however that $\alpha \sim -\ln t$ appears at sufficiently low temperatures for $t \lesssim 10^{-4}$, as shown in Fig. 5(b). This is due to the temperature dependence of $(\frac{\partial y}{\partial P})_T$ in α_b in Eq. (70), as noted above. As shown in Fig. 5(a), $\alpha(t)$ shows a slight increase down to $t \sim 10^{-2}$, which is seen as almost flat- t behavior, and divergent- t behavior becomes visible for lower temperatures $t \lesssim 10^{-2}$.

Note that although α diverges for $t \rightarrow 0$, the entropy becomes zero, i.e., $S \rightarrow 0$, for $t \rightarrow 0$, which is confirmed with the use of Eq. (39), satisfying the third law of thermodynamics. This can also be seen by integrating αV with respect to P [see Eq. (5)] as [17]

$$S(P, T) = S(P_c, T) - \int_{P_c}^{P^*} \alpha V dP' - \int_{P^*}^P \alpha V dP', \quad (103)$$

where P_c denotes the QCP and P^* characterizes the crossover from the quantum-critical to Fermi-liquid regimes. Let us consider the case for $P > P^*$ that $S(P, T)$ and the last term of the r.h.s. in Eq. (103) are in the Fermi-liquid regime, both of which vanish for $t \rightarrow 0$. Since $y(t=0)$ has a finite slope at $P = P_c$, i.e., $(\frac{\partial y}{\partial P})_{T=0} \neq 0$, the crossover line in the P - t phase diagram behaves as $P^* - P_c \sim (\frac{\partial P}{\partial y})_{T=0} t^{2/3}$. Here $t^{2/3}$ is the crossover temperature between the quantum-critical region and the Fermi-liquid region in the P - t phase diagram, where $y/t^{2/z}$ much smaller (larger) than 1 for $t \rightarrow 0$ gives the quantum-critical (Fermi-liquid) region [see Eq. (B4) in Appendix B]. Then, the second term on the r.h.s. of Eq. (103) becomes zero for $t \rightarrow 0$ since the integration region

vanishes as $P^* - P_c \sim t^{2/3} \rightarrow 0$ over which α is divergent as Eq. (102). This yields $S(P_c, T \rightarrow 0) = 0$.

D. 2D antiferromagnetic case

Figure 6(a) shows the temperature dependence of the thermal-expansion coefficient α at the AFM QCP ($z = 2$) in $d = 2$. As t decreases, α_b in Eq. (68) contributes to α dominantly, $\alpha \approx \frac{1}{V} \frac{\tilde{C}_b}{t} (\frac{\partial y}{\partial P})_T$, while contribution from α_a becomes not negligible as t increases.

In Eq. (95) for $d + z = 4$, we estimate $\frac{y_1}{2}(y \ln y + 2L) = y \approx -\frac{t \ln(-\ln t)}{2 \ln t}$ [see Eq. (34) and Appendix D], $\tilde{C}_b \sim t \ln(-\ln t)$ [Eq. (59)], and $M \sim t \frac{\ln t}{\ln(-\ln t)}$ for $t \ll 1$. Hence, we have $(\frac{\partial y}{\partial P})_T / (\frac{\partial y_0}{\partial P})_{T=0} \approx -b_4 / \ln(-\frac{t}{\ln t})$ with b_4 being a positive constant. Note that divergence of the denominator of Eq. (95) occurs because the $\ln y$ and M terms diverge for $t \rightarrow 0$ and then we have $\lim_{T \rightarrow 0} (\frac{\partial y}{\partial P})_T = 0$ irrespective of the input values of $(\frac{\partial y_0}{\partial P})_{T=0}$ in Eq. (95). This can be confirmed by the numerical calculation of Eq. (95), which is shown in the inset of Fig. 6(b).

For $t \ll 1$, α behaves as

$$\alpha \propto \frac{\tilde{C}_b}{t} \left(\frac{\partial y}{\partial P} \right)_T \sim -\frac{\ln(-\ln t)}{\ln(-\frac{t}{\ln t})}, \quad (104)$$

where $\frac{\tilde{C}_b}{t} (\frac{\partial y}{\partial P})_T \sim -\frac{\ln(-\ln t)}{\ln(-\frac{t}{\ln t})}$ dominates over $C_a \sim -t \ln t$ [Eq. (60)] in Eq. (68). Although Eq. (104) gives the accurate expression of α for $t \ll 1$, here taking the leading term of the denominator, we plot $\alpha \sim -\frac{\ln(-\ln t)}{\ln t}$ in Fig. 6(b) as a dashed line, which well reproduces α_b and also α for $t < 10^{-2}$. It is noted that the low-temperature behavior $\ln(-\ln t)$ in Eq. (104) coincides with the temperature dependence of the critical part shown by the RG theory [17] except for the prefactor $(\frac{\partial y}{\partial P})_T$, which gives the $-\ln(-\frac{t}{\ln t})$ contribution to the denominator of Eq. (104) [36].

The temperature dependence of α for $t \ll 1$ at the QCP for each class is summarized in Table II.

It is noted that Takahashi derived $\alpha(t)$ from the volume derivative of the free energy in the extended SCR theory by introducing the conservation law of the total spin fluctuation amplitude and discussed the 3D FM case with finite transition

TABLE II. Temperature dependence of the thermal-expansion coefficient α and the Grüneisen parameter Γ just at the QCP for each class specified by $z = 3$ (FM) and $z = 2$ (AFM) in $d = 3$ and 2.

Class	α	Γ
3D FM	$T^{1/3}$	$-\frac{T^{-2/3}}{\ln T}$
3D AFM	$T^{1/2}$	$\frac{T^{-1/2}}{\text{const.} - T^{1/2}}$
2D FM	$-\ln T$	$-T^{-2/3} \ln T$
2D AFM	$-\frac{\ln(-\ln T)}{\ln(-\frac{T}{\ln T})}$	$\frac{1}{T \ln T} \frac{\ln(-\ln T)}{\ln(-\frac{T}{\ln T})}$

temperatures [28]. The present study has shown that $\alpha(t)$ derived from the volume derivative of the SCR free energy (Sec. VC) is equivalent to $\alpha(t)$ derived from the pressure derivative of the SCR entropy (Sec. VA). On the basis of the latter result, which has a much simpler expression, the critical properties of $\alpha(t)$ at the QCP for each class ($z = 3, 2$ in $d = 3, 2$) have been clarified.

VII. NUMERICAL RESULTS ON GRÜNEISEN PARAMETER Γ AT THE MAGNETIC QCP

The Grüneisen parameter Γ is defined by Eq. (6). On the other hand, Γ in the adiabatic process has been derived in Sec. IV, whose explicit form is given by Eq. (65). It can be shown that for $t \rightarrow 0$ the former expression is equivalent to the latter one as follows:

Let us consider Eq. (6). Near the magnetic QCP, the thermal-expansion coefficient α is given in Eq. (68) and the specific heat C_V is given in Eq. (40). As shown in Sec. III, for $t \ll 1$, the dominant contribution to C_V comes from C_a as $C_V = C_a - C_b \approx C_a$. Hence, Γ is expressed for $t \ll 1$ as

$$\begin{aligned} \Gamma &\approx \frac{\tilde{C}_b}{C_a} \frac{1}{t} \frac{1}{\kappa_T} \left(\frac{\partial y}{\partial P} \right)_T + \frac{1}{\kappa_T} \frac{1}{T_0} \left(\frac{\partial T_0}{\partial P} \right)_T \\ &= -\frac{\tilde{C}_b}{C_a} \frac{V}{t} \left(\frac{\partial y}{\partial V} \right)_T - \frac{V}{T_0} \left(\frac{\partial T_0}{\partial V} \right)_T, \end{aligned} \quad (105)$$

where κ_T defined in Eq. (4) has been used to derive the second line. Since T_0 defined in Eq. (25) is the quantity at $T = 0$ and does not depend on T , we have $(\frac{\partial T_0}{\partial V})_T = (\frac{\partial T_0}{\partial V})_S$. For sufficiently low temperatures, $(\frac{\partial y}{\partial V})_T$ at a constant T can be approximated as the one at a constant S , i.e., $(\frac{\partial y}{\partial V})_T \approx (\frac{\partial y}{\partial V})_S$. Then, it is confirmed explicitly for $t \ll 1$ that Eq. (105) coincides with Eq. (65).

Here we remark the property of the isothermal compressibility κ_T defined by Eq. (4). By differentiating the pressure P in Eq. (72) with respect to the volume V under a constant temperature T , $(\frac{\partial P}{\partial V})_T$ can be calculated as discussed in Sec. VC. It can be shown that the $t \rightarrow 0$ limit of $(\frac{\partial P}{\partial V})_T$ is finite but not zero at the QCP for each class specified by $z = 3$ and 2 in $d = 3$ and 2. Hence, the $t \rightarrow 0$ limit of the isothermal compressibility is finite at the QCP, i.e., $\lim_{t \rightarrow 0} \kappa_T = \text{const.}$

In the following subsections the temperature dependence of Γ at the QCP for each class will be analyzed on the basis of Eq. (6). The specific heat C_V in Eq. (40) is calculated by the procedure in Sec. III and the thermal-expansion coefficient α

in Eq. (68) is calculated by the procedure in Sec. VI. With the use of Eq. (68), Γ is expressed as

$$\Gamma = \Gamma_a + \Gamma_b, \quad (106)$$

where Γ_i is defined by

$$\Gamma_i \equiv \frac{\alpha_i V}{C_V \kappa_T}, \quad (107)$$

for $i = a, b$. For $t \ll 1$, Γ_a and Γ_b lead to the second and first terms in Eq. (105), respectively. To plot the t dependence of Γ , here we input $\kappa_T = 0.1$ as a representative value (the reason for this parametrization is explained below), although given the first and second derivatives of T_0 , T_A , v_4 , and $\eta_0/(Aq_B^2)$ with respect to V , the temperature dependence of κ_T can be computed explicitly. Other input parameters are the same as those set in Figs. 2 and 3.

Here we comment on the parametrization. The Grüneisen parameter $\Gamma_a(T = 0) = -\frac{V}{T_0} (\frac{\partial T_0}{\partial V})_{T=0}$ in heavy electron systems is estimated to be in the same order of $-\frac{V}{T_K} (\frac{\partial T_K}{\partial V})_{T=0}$, with T_K being the characteristic temperature called Kondo temperature, which typically has an enhanced value of $O(10)$, as will be shown in Sec. IX C [see Eq. (120)]. Since $\frac{1}{T_0} (\frac{\partial T_0}{\partial P})_T = \Gamma_a(T = 0) \kappa_T = 1.0$ was used in Sec. VI as a typical input value, here we input $\kappa_T = 0.1$ as a typical value for the heavy electron system, giving rise to $\Gamma_a(T = 0) = 10.0$.

If one makes a comparison with the system with the normal metal where the Grüneisen parameter is not enhanced in the Fermi-liquid region but has the value of $O(1)$ (e.g., d electron systems), κ_T of $O(1)$ is to be input for $\frac{1}{T_0} (\frac{\partial T_0}{\partial P})_T = 1.0$, which gives $\Gamma_a(T = 0)$ of $O(1)$. Hence the vertical scales of the following Figs. 7–10 are an order of magnitude smaller in that case.

To make more explicit comparison with experiments, the bulk modulus κ_T^{-1} in the unit of GPa for each material is multiplied to $\frac{1}{T_0} (\frac{\partial T_0}{\partial P})_T$ in the unit of GPa^{-1} [see Eqs. (98) and (99)], giving rise to the dimensionless Γ_a . These values can actually be determined from the measurements, which will be discussed in Sec. IX C 1.

A. 3D ferromagnetic case

Figure 7(a) shows the temperature dependence of the Grüneisen parameter Γ at the FM QCP ($z = 3$) in $d = 3$. As t decreases, Γ increases and diverges at the ground state, which is mainly contributed from Γ_b . For $t \ll 1$, the thermal-expansion coefficient is evaluated as $\alpha \approx \alpha_b \sim t^{1/3}$ in Eq. (100) and the specific heat is evaluated as $C_V \approx C_a \sim -t \ln t$ in Eq. (49). Then, Γ is evaluated as

$$\Gamma \approx \Gamma_b \sim -\frac{t^{-3/2}}{\ln t}, \quad (108)$$

for $t \ll 1$. This is numerically confirmed in Fig. 7(b), where $\Gamma(t)(-\ln t)$ (thick solid line) behaves as $\sim t^{-2/3}$ (dashed line) for $t \ll 1$. The behavior of Eq. (108) is in accord with the RG theory [17], which appears at sufficiently low temperatures for $t \lesssim 10^{-4}$, as shown in Fig. 7(b).

In the Curie-Weiss regime [see Fig. 1(a)], $\Gamma(t)$ shows a monotonic decrease as t increases. The least-square fit of $1/\Gamma(t)$ in the form of at^γ for $0.07 \leq t \leq 0.20$ gives $\gamma =$

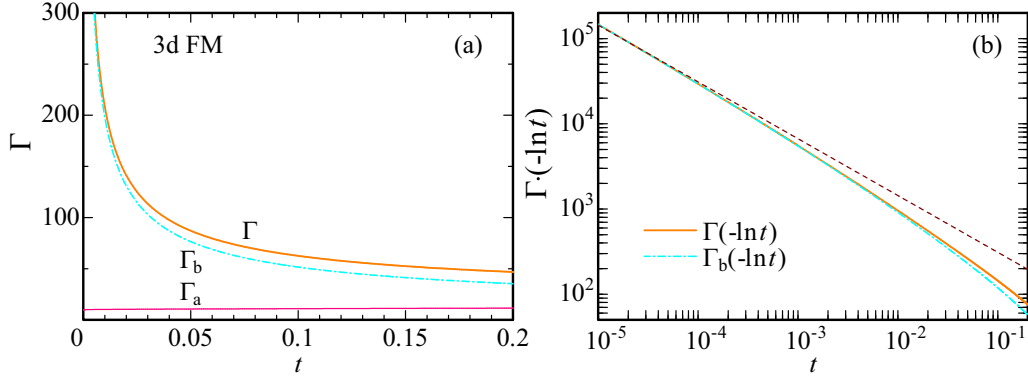


FIG. 7. (a) Temperature dependence of the Grüneisen parameter Γ (thick solid line), Γ_a (thin solid line), and Γ_b (dash-dotted line) at the 3D FM QCP. (b) Temperature dependence of $\Gamma(-\ln t)$ (thick solid line) and $\Gamma_b(-\ln t)$ (dash-dotted line). The dashed line represents the least-square fit of $\Gamma(-\ln t)$ with $at^{-2/3}$ for $10^{-5} \leq t \leq 10^{-4}$.

0.43. Hence, $\Gamma(t)$ behaves as $\Gamma(t) \sim t^{-0.43}$ in the Curie-Weiss regime.

B. 3D antiferromagnetic case

Figure 8(a) shows the temperature dependence of the Grüneisen parameter Γ at the AFM QCP ($z = 2$) in $d = 3$. As t decreases, Γ increases and diverges at the ground state, which is mainly contributed from Γ_b . For $t \ll 1$, the thermal-expansion coefficient is evaluated as $\alpha \approx \alpha_b \sim t^{1/2}$ in Eq. (101) and the specific heat is evaluated as $C_V \approx C_a \sim t(\text{const.} - t^{1/2})$ in Eq. (52). Then Γ is evaluated as

$$\Gamma \approx \Gamma_b \sim \frac{t^{-1/2}}{\text{const.} - t^{1/2}}, \quad (109)$$

for $t \ll 1$. This is numerically confirmed in Fig. 8(b), where $\Gamma(t)(\frac{1}{2} - t^{1/2})$ (thick solid line) behaves as $\sim t^{-1/2}$ (dashed line) for low t . The behavior of Eq. (109) is in accord with the RG theory [17], which appears at sufficiently low temperatures for $t \lesssim 10^{-4}$, as shown in Fig. 8(b).

As for the Curie-Weiss regime [see Fig. 1(b)], the least-square fit of $1/\Gamma(t)$ in the form of at^γ in the Curie-Weiss regime for $0.07 \leq t \leq 0.20$ gives $\gamma = 0.43$. Hence, $\Gamma(t)$ behaves as $\Gamma(t) \sim t^{-0.43}$ in the Curie-Weiss regime.

C. 2D ferromagnetic case

Figure 9(a) shows the temperature dependence of the Grüneisen parameter Γ at the FM QCP ($z = 3$) in $d = 2$. As t decreases, Γ increases and diverges at the ground state, which is mainly contributed from Γ_b . For $t \ll 1$, the thermal-expansion coefficient is evaluated as $\alpha \approx \alpha_b \sim -\ln t$ in Eq. (102) and the specific heat is evaluated as $C_V \approx C_a \sim t^{2/3}$ in Eq. (56). Then, Γ is evaluated as

$$\Gamma \approx \Gamma_b \sim -t^{-2/3} \ln t, \quad (110)$$

for $t \ll 1$. This is numerically confirmed in Fig. 9(b), where $\Gamma(t)/(-\ln t)$ (thick solid line) behaves as $\sim t^{-2/3}$ (dashed line) for low t . The behavior of Eq. (110) is in accord with the RG theory [17], which appears at sufficiently low temperatures for $t \lesssim 10^{-4}$, as shown in Fig. 9(b).

As for the Curie-Weiss regime [see Fig. 1(c)], the least-square fit of $1/\Gamma(t)$ in the form of at^γ in the Curie-Weiss regime for $0.07 \leq t \leq 0.20$ gives $\gamma = 0.50$. Hence, $\Gamma(t)$ behaves as $\Gamma(t) \sim t^{-0.50}$ in the Curie-Weiss regime.

D. 2D antiferromagnetic case

Figure 10(a) shows the temperature dependence of the Grüneisen parameter Γ at the AFM QCP ($z = 2$) in $d = 2$.

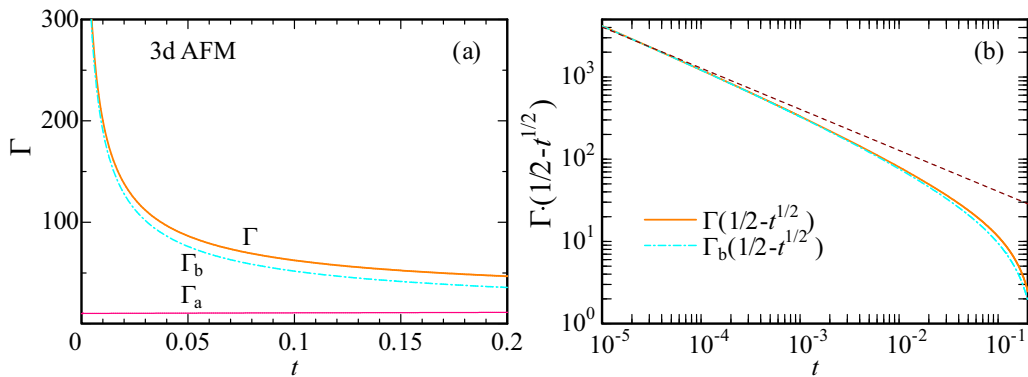


FIG. 8. (a) Temperature dependence of the Grüneisen parameter Γ (thick solid line), Γ_a (thin solid line), and Γ_b (dash-dotted line) at the 3D AFM QCP. (b) Temperature dependence of $\Gamma(\frac{1}{2} - t^{1/2})$ (thick solid line) and $\Gamma_b(\frac{1}{2} - t^{1/2})$ (dash-dotted line). The dashed line represents the least-square fit of $\Gamma(\frac{1}{2} - t^{1/2})$ with $at^{-1/2}$ for $10^{-5} \leq t \leq 10^{-4}$.

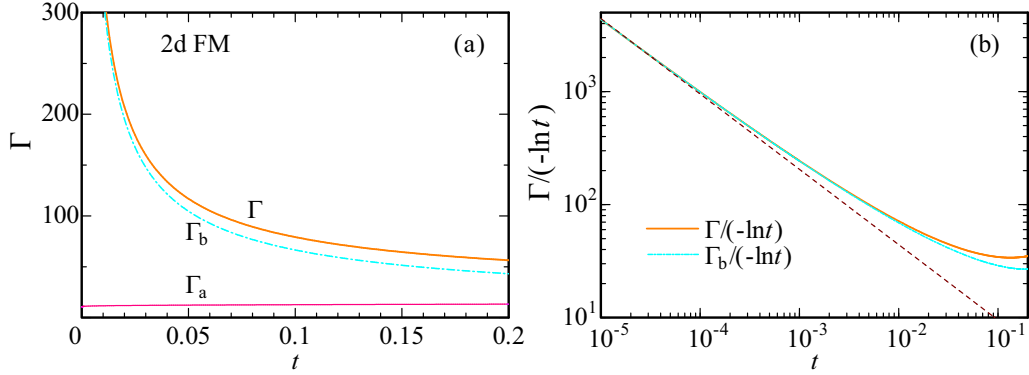


FIG. 9. (a) Temperature dependence of the Grüneisen parameter Γ (thick solid line), Γ_a (thin solid line), and Γ_b (dash-dotted line) at the 2D FM QCP. (b) Temperature dependence of $\Gamma/(-\ln t)$ (thick solid line) and $\Gamma_b/(-\ln t)$ (dash-dotted line). The dashed line represents the least-square fit of $\Gamma/(-\ln t)$ with $at^{-2/3}$ for $10^{-5} \leq t \leq 10^{-4}$.

As t decreases, Γ increases and diverges at the ground state, which is mainly contributed from Γ_b . For $t \ll 1$, the thermal-expansion coefficient is evaluated in Eq. (104), whose precise form is $\alpha \approx \alpha_b \sim -\frac{\ln(-\ln t)}{\ln(-\frac{t}{\ln t})}$. The specific heat is evaluated as $C_V \approx C_a \sim -t \ln t$ in Eq. (60). Then, Γ is evaluated as

$$\Gamma \approx \Gamma_b \sim \frac{1}{t} \frac{\ln(-\ln t)}{\ln t \ln\left(-\frac{t}{\ln t}\right)}, \quad (111)$$

for $t \ll 1$. This is confirmed in Fig. 10(b), where $\Gamma(t)t(-\ln t)$ (thick solid line) behaves as $\sim -\frac{\ln(-\ln t)}{\ln(-\frac{t}{\ln t})}$ (dashed line) for low t . The behavior of Eq. (111) agrees with the critical part shown by the RG theory [17] except for $\ln(-\frac{t}{\ln t})$ in the denominator, which arises from the prefactor $(\partial y/\partial P)_T$ in α_b as discussed in Sec. VID [36].

As for the Curie-Weiss regime [see Fig. 1(d)], the least-square fit of $1/\Gamma(t)$ in the form of at^γ in the Curie-Weiss regime for $0.07 \leq t \leq 0.20$ gives $\gamma = 0.41$. Hence, $\Gamma(t)$ behaves as $\Gamma(t) \sim t^{-0.41}$ in the Curie-Weiss regime.

The temperature dependence of Γ for $t \ll 1$ at the QCP for each class is summarized in Table II.

VIII. NUMERICAL RESULTS ON GRÜNEISEN PARAMETER Γ NEAR THE MAGNETIC QCP

In this section we discuss the Grüneisen parameter near the QCP for each class on the basis of the SCR theory. We calculate $\Gamma(t)$ in the paramagnetic phase by solving the SCR equation (33) for $d+z > 4$ and Eq. (34) for $d+z = 4$ in the paramagnetic region ($y_0 > 0$) and also in the region where the magnetic order takes place ($y_0 < 0$). The input parameters other than y_0 are the same as those in Sec. VII. The results are shown in Figs. 11(a)–11(d) [see corresponding Figs. 1(a)–1(d), respectively].

At the QCP specified by $y_0 = 0$, $\Gamma(t)$ shows the divergence for $t \rightarrow 0$ in each class. As getting away from the QCP in the paramagnetic region, $\Gamma(t)$ for $t \rightarrow 0$ becomes finite, whose value decreases as y_0 increases from 0, as shown in Figs. 11(a)–11(d).

On the other hand, as y_0 decreases from 0, the magnetic order occurs at finite temperature $t = t_c \equiv T_c/T$ for 3D FM [Fig. 11(a)] and 3D AFM [Fig. 11(b)]. In the high- t regime for $t \gtrsim 0.7$, $\Gamma(t)$ shows the Curie-Weiss behavior in each class as mentioned above. As t decreases, $\Gamma(t)$ increases and turns to decrease, which finally converges into a finite value

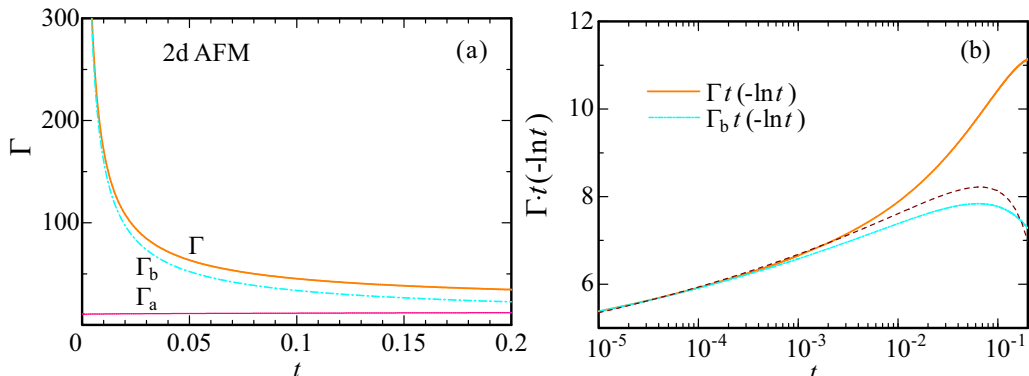


FIG. 10. (a) Temperature dependence of the Grüneisen parameter Γ (thick solid line), Γ_a (thin solid line), and Γ_b (dash-dotted line) at the 2D AFM QCP. (b) Temperature dependence of $\Gamma t(-\ln t)$ (thick solid line) and $\Gamma_b t(-\ln t)$ (dash-dotted line). The dashed line represents the least-square fit of $\Gamma t(-\ln t)$ with $-a \frac{\ln(-\ln t)}{\ln(-\frac{t}{\ln t})}$ for $10^{-5} \leq t \leq 10^{-4}$.

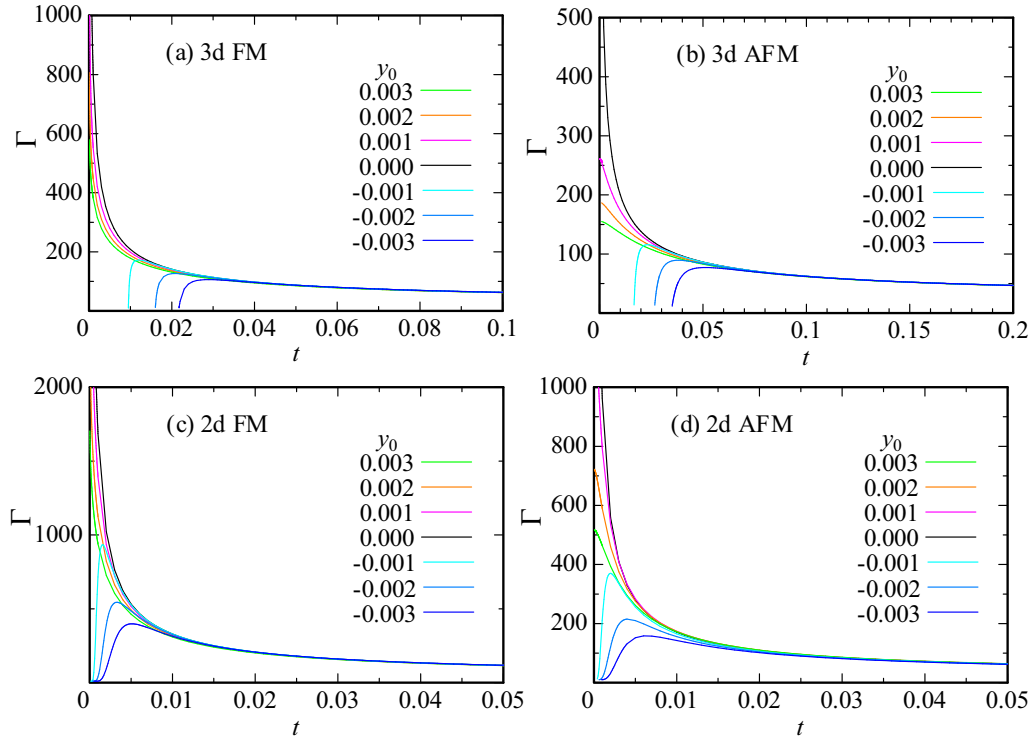


FIG. 11. Scaled temperature dependence of the Grüneisen parameter for (a) 3D FM, (b) 3D AFM, (c) 2D FM, and (d) 2D AFM.

$\Gamma(t) \rightarrow \Gamma_a(t = t_c) = -\frac{V}{T_0} \left(\frac{\partial T_0}{\partial V} \right)_{T=T_c} = 10.0$ for $t \rightarrow t_{c+}$. This is because $\tilde{C}_b \rightarrow 0$ is realized for $y \rightarrow 0$ as t approaches t_c from the high- t side, making $\alpha_b \propto \frac{\tilde{C}_b(t_c)}{t_c} \rightarrow 0$ in Eq. (70). Then, by Eq. (106), it turns out that the Grüneisen parameter at t_c is expressed as $\Gamma(t) \rightarrow \Gamma_a(t)$ for $t \rightarrow t_{c+}$.

For 2D FM and 2D AFM, the magnetic order occurs only at $t = t_c = 0$. The Grüneisen parameters for $y_0 < 0$ in this case also show $\Gamma(t) \rightarrow \Gamma_a(t) = -\frac{V}{T_0} \left(\frac{\partial T_0}{\partial V} \right)_{T=0} = 10.0$ for $t \rightarrow 0_+$, as seen in Figs. 11(c) and 11(d), respectively.

IX. DISCUSSION

A. Divergence of the Grüneisen parameter and the characteristic energy scale at the QCP

In the SCR theory, the characteristic temperature of spin fluctuation T_0 is not zero even at the QCP in general, as will be illustrated in Fig. 12. In Sec. VII it was shown that the Grüneisen parameter Γ diverges at the magnetic QCP for each class ($z = 3, 2$ in $d = 3, 2$). The origin of the divergence can be traced back to the entropy of the SCR theory. The entropy S is expressed as the scaled form in Eq. (39) with a variable u defined by Eq. (31). The volume dependence arises from y in the numerator and T_0 in the denominator of Eq. (31), which lead to the first and second terms in Eq. (65), respectively. The former gives rise to the divergence of Γ for $t \rightarrow 0$ at the QCP and the latter gives the V derivative of the characteristic temperature T_0 [see Eq. (65) or (105)]. The present study has clarified that the inverse susceptibility (renormalized by the mode-mode coupling of spin fluctuations) coupled to V gives rise to the divergence of Γ in addition to the ordinary contri-

bution from the V derivative of the characteristic temperature of the system.

The temperature dependence of the dominant term of the thermal-expansion coefficient α and Γ for $t \ll 1$ coincides with the critical part shown by the RG theory [17] except for the temperature dependent $\left(\frac{\partial y}{\partial P} \right)_T$ in α and Γ for $z = 2$ in $d = 2$ (see Secs. VID and VIID). In Ref. [17], the Grüneisen parameter defined by $\Gamma \equiv \alpha/C_P$ was analyzed and the relation $\Gamma \sim T^{-\frac{1}{\nu z}}$ was derived by assuming the hyperscaling relation, which is generally justified only below the upper critical dimension ($d + z < 4$) within the Φ^4 theory [see Eq. (11)]. Here ν is the exponent for the correlation length $\xi \sim |r|^{-\nu}$ with $r \equiv (P - P_c)/P_c$. The results in Sec. VII are obtained above ($d + z > 4$) and just at the upper critical dimension ($d + z = 4$). For comparison, let us reexpress the specific heat C_V , α , and Γ in terms of d and z for each class in the following subsections.

1. 3D ferromagnetic case ($d = 3, z = 3$)

For $t \ll 1$, the specific heat [Eq. (49)] is expressed as $C_V \approx C_a \sim -t^{\frac{d}{z}} \ln t$. The thermal expansion coefficient α [Eq. (100)] is expressed as $\alpha \approx \alpha_b \sim t^{\frac{d-2}{z}}$. Then, the Grüneisen parameter [Eq. (108)] is expressed as

$$\Gamma \approx \frac{\alpha}{C_V} \sim -\frac{t^{-\frac{2}{z}}}{\ln t}. \quad (112)$$

2. 3D antiferromagnetic case ($d = 3, z = 2$)

For $t \ll 1$, the specific heat [Eq. (52)] is expressed as $C_V \approx C_a \sim t^{\frac{d-1}{z}}$ (const. $-t^{\frac{d-1}{z}}$). The thermal expansion coefficient α [Eq. (101)] is expressed as $\alpha \approx \alpha_b \sim t^{\frac{d-2}{z}}$. Then,

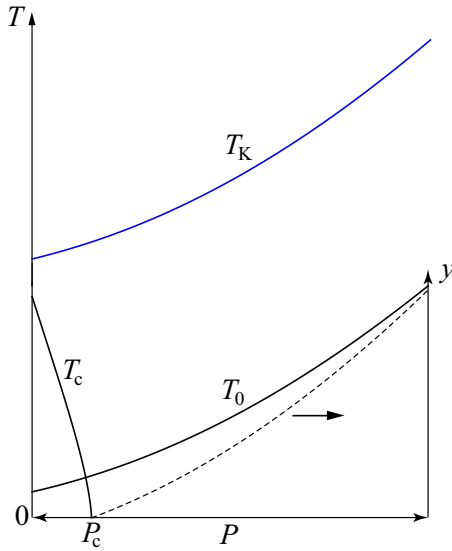


FIG. 12. Schematic temperature-pressure phase diagram of Ce-based heavy-electron systems (right-pointing P axis) and Yb-based heavy-electron systems (left-pointing P axis) in $d = 3$. The Kondo temperature T_K and the characteristic temperature of spin fluctuation T_0 are given by the solid lines (left axis). Note that vertical scales for T_K and T_0 can be different in general. Depending on the parameters in each material, it is possible that $T_0(P)$ gets close to $T_K(P)$ (see text). The magnetic transition temperature T_c (solid line, left axis) is suppressed to 0 at the QCP denoted by P_c . The dashed line gives $y = 1/[2T_A\chi_Q(0, 0)]$ (right axis) for $P > P_c$. Note that in $d = 2$ for $z = 2$ the dashed line starts to appear from P_c with a vanishing slope $(\frac{\partial y}{\partial P})_{T=0} = 0$ (see Sec. VID). Note that it is possible that a crossing of $T_K(P)$ and $T_c(P)$ occurs depending on the material parameters. If the system has XY or Heisenberg symmetry, no magnetic transition occurs for finite T in $d = 2$.

the Grüneisen parameter [Eq. (109)] is expressed as

$$\Gamma \approx \frac{\alpha}{C_V} \sim \frac{t^{\frac{d-2}{z}}}{t^{\frac{d-1}{z}} (\text{const.} - t^{\frac{d-1}{z}})}. \quad (113)$$

3. 2D ferromagnetic case ($d = 2, z = 3$)

For $t \ll 1$, the specific heat [Eq. (56)] is expressed as $C_V \approx C_a \sim t^{\frac{d}{z}}$. The thermal expansion coefficient α [Eq. (102)] is expressed as $\alpha \approx \alpha_b \sim -\ln t$. Then, the Grüneisen parameter [Eq. (110)] is expressed as

$$\Gamma \approx \frac{\alpha}{C_V} \sim -\frac{t^{-\frac{d}{z}}}{\ln t}. \quad (114)$$

4. 2D antiferromagnetic case ($d = 2, z = 2$)

For $t \ll 1$, the specific heat [Eq. (60)] is expressed as $C_V \approx C_a \sim -t^{\frac{d}{z}} \ln t$. The thermal expansion coefficient α [Eq. (104)] is expressed precisely as $\alpha \approx \alpha_b \sim -\ln(-\ln t)/\ln(-\frac{t}{\ln t})$. Then, the Grüneisen parameter [Eq. (111)] is expressed as

$$\Gamma \approx \frac{\alpha}{C_V} \sim \frac{t^{-\frac{d}{z}} \ln(-\ln t)}{\ln t \ln(-\frac{t}{\ln t})}. \quad (115)$$

In Eqs. (112), (114), and (115), Γ has the t dependence as $t^{-2/z}$ with logarithmic corrections. In Eq. (113), if the first

term of the denominator is neglected, Γ has the t dependence as $t^{-\frac{d-1}{z}}$, which is also expressed as $t^{-2/z}$. Since the dynamical magnetic susceptibility with the quadratic momentum dependence in Eq. (21) yields $\nu = 1/2$ in the SCR theory, as a result, all these t dependence can be expressed as $t^{-\frac{1}{\nu z}}$ except for the logarithmic corrections.

B. Comparison with the Moriya-Usami theory

Moriya and Usami discussed the magnetovolume effect in nearly ferromagnetic metals [15] on the basis of the volume strain $\omega_m \equiv \frac{\delta V}{V}$ expressed as

$$\omega_m(T) - \omega_m(T_c) \propto y, \quad (116)$$

for $T > T_c$, where T_c is the ferromagnetic-transition temperature. The volume strain in nearly antiferromagnetic metals was also discussed on the basis of Eq. (116) where T_c is the Néel temperature [13]. Since the thermal-expansion coefficient α is obtained by $\alpha = \frac{d\omega_m}{dT}$ according to its definition in Eq. (1), Eq. (116) indicates that α is proportional to $\frac{dy}{dT}$, i.e., $\alpha \propto \frac{dy}{dT}$.

It should be noted here that Eq. (116) was *not* shown to be derived from the free energy [13,15,28]. In this paper, we have derived the thermal-expansion coefficient α starting from the free energy (or equivalently from the entropy) in the SCR theory with the use of the stationary condition adequately, which results in Eq. (68). Then we have obtained $\alpha \approx \alpha_b \sim \frac{\tilde{C}_b}{t} (\frac{\partial y}{\partial P})_T$ for $t \ll 1$ at the QCP, as shown in Sec. VI. Hence, let us compare our result with the Moriya-Usami theory at $T_c = 0$.

For $d + z > 4$, the temperature dependence of y and \tilde{C}_b is the same for $t \ll 1$, and $(\frac{\partial y}{\partial P})_T \sim \text{const.}$ for $t \rightarrow 0$, as shown in Secs. VIA, VIB, and VIC. Hence, it turns out that $\frac{\tilde{C}_b}{t} (\frac{\partial y}{\partial P})_T$ has the same temperature dependence as $\frac{dy}{dT}$ for $t \ll 1$.

For $d + z = 4$, the temperature dependence of $y \sim -\frac{t \ln(-\ln t)}{\ln t}$ and $\tilde{C}_b \sim t \ln(-\ln t)$ for $t \ll 1$ are different. However, $(\frac{\partial y}{\partial P})_T$ has the temperature dependence as $(\frac{\partial y}{\partial P})_T \sim -[\ln(-\frac{t}{\ln t})]^{-1}$ for $t \ll 1$, as shown in Sec. VID. Hence, $\frac{\tilde{C}_b}{t} (\frac{\partial y}{\partial P})_T$ is expressed as $\sim -\frac{\ln(-\ln t)}{\ln(-\frac{t}{\ln t})}$. This still looks different from $\frac{dy}{dT} \sim -\frac{\ln(-\ln t)}{\ln t}$. However, at low temperatures $\frac{\tilde{C}_b}{t} (\frac{\partial y}{\partial P})_T$ can be approximated as $\sim -\frac{\ln(-\ln t)}{\ln t}$, which was confirmed numerically as shown in Fig. 6(b). Thus, it can be regarded that in practice $\frac{\tilde{C}_b}{t} (\frac{\partial y}{\partial P})_T$ has the same temperature dependence as $\frac{dy}{dT} \sim -\frac{\ln(-\ln t)}{\ln t}$ as far as the leading term is concerned.

Hence, as a consequence, our result in Eq. (68) and Moriya-Usami's $\alpha \propto \frac{dy}{dT}$ give the same (practically the same) t dependence of α for $t \ll 1$ for $d + z > 4$ ($d + z = 4$). This can be seen immediately by comparing $\frac{dy}{dT} \propto \frac{d\eta}{dT}$ in Table I with $\alpha(t)$ in Table II for each class. Note that behavior in Table II appears at sufficiently low temperatures as shown in Figs. 3–6, and hence $\alpha \propto \frac{dy}{dT}$ does not hold at temperatures except for $t \ll 1$.

C. Comparison with experiments

The thermal-expansion coefficient is generally expressed as

$$\alpha = \alpha_e + \alpha_{\text{ph}} + \alpha_{\text{mag}}, \quad (117)$$

where α_e and α_{ph} are contributions from itinerant electrons and acoustic phonons, respectively. At low temperatures, α_e behaves as $\alpha_e = aT$, as shown by the free-electron model, and α_{ph} is given by $\alpha_{\text{ph}} = \beta T^3$ [37]. In Eq. (117), α_{mag} arises from spin fluctuations, which become profound near the continuous magnetic-transition point, as discussed in Sec. V (note that α_{mag} was denoted as α in Sec. V).

The Grüneisen parameter is generally expressed as

$$\Gamma = \Gamma_e + \Gamma_{\text{ph}} + \Gamma_{\text{mag}}, \quad (118)$$

where Γ_i is defined by Eq. (107) with $i = e, \text{ph}, \text{and mag}$, corresponding to each term in Eq. (117). For sufficiently lower temperatures than the Fermi temperature, Γ_e is given as a constant [37]. In heavy electron systems, the characteristic temperature of the quasiparticles is the effective Fermi temperature, which is referred to as the Kondo temperature T_K in the lattice system. Then, the characteristic temperature T^* in Eq. (8) is set to be T_K , which leads to [29,38,39]

$$\Gamma_e = -\frac{V}{T_K} \left(\frac{\partial T_K}{\partial V} \right)_S. \quad (119)$$

To grasp the main property, let us take the view from the strong limit of on-site Coulomb repulsion of f electrons. By inputting $T_K = De^{-\frac{1}{N_{\text{CF}}J}}$ to Eq. (119), where D and N_{CF} are the half-band width and the density of states at the Fermi level of conduction electrons per “spin,” respectively, and J is the effective Kondo exchange coupling ($J > 0$) in the lattice system [40,41], we obtain for $N_{\text{CF}}J \ll 1$

$$\Gamma_e \approx -\frac{1}{N_{\text{CF}}J} \left\{ \frac{V}{J} \left(\frac{\partial J}{\partial V} \right)_S + c \right\}, \quad (120)$$

where c is a constant of $O(1)$ (e.g., $c = 2/3$ for free conduction electrons in $d = 3$). In heavy electron systems, $(JN_{\text{CF}})^{-1}$ typically has a magnitude of $O(10)$. Thus we see that the factor $(N_{\text{CF}}J)^{-1}$ gives rise to the enhancement of $|\Gamma_e|$, which is often observed in the heavy electron metals with about 10–100 times larger values than those of ordinary metals [29,39,42,43].

When the system approaches the continuous magnetic-transition point by varying parameters, e.g., by applying pressure or magnetic field, or chemical doping, Γ_{mag} arising from spin fluctuations becomes predominant in Eq. (118), as discussed in Sec. VII (note that Γ_{mag} was denoted as Γ in Sec. VII). In the following subsections, let us discuss the pressure tuning to the magnetic QCP in the Ce- and Yb-based heavy electron systems.

1. Pressure effects on Ce-based systems

In the Ce-based heavy electron systems, by applying pressure, the hybridization between f and conduction electrons $|V_{fc}|$ increases and the f level ε_f increases in general. Hence, the Kondo coupling $J \sim \frac{V_{fc}^2}{\varepsilon_F - \varepsilon_f}$ increases, giving rise to increase in the Kondo temperature T_K . This yields $(\frac{\partial J}{\partial V})_S < 0$, which leads to $\Gamma_e > 0$ in Eq. (120) [44].

Namely, the system becomes more itinerant under pressure, which makes the characteristic temperature of spin fluctuation T_0 increase. Direct evaluation of T_0 in Eq. (25) gives $T_0 = \tilde{A}v_F\tilde{q}_B/(\pi^2n^{2/3})$ in $d = 3$, where v_F is the Fermi

velocity and n is the filling defined by $n \equiv \frac{N_c}{2N}$. Here \tilde{q}_B is given by $\tilde{q}_B = q_B$ for $z = 3$ and $\tilde{q}_B = Q$ for $z = 2$, and \tilde{A} is a dimensionless constant defined by the q^2 coefficient around the ordered vector \mathbf{Q} in the irreducible susceptibility at $\omega = 0$ (e.g., $\tilde{A} = \frac{1}{12}$ for the free electron model [7]). Since $v_F \sim T_K$ holds, applying pressure induces an increase in v_F reflecting the pressure-induced expansion of the effective bandwidth of the quasiparticles. This effect contributes to increase in T_0 under pressure, i.e., $(\frac{\partial T_0}{\partial P}) > 0$.

Indeed, in Ce_7Ni_3 , it was observed that T_0 increases as pressure increases [48]. Moreover, smooth variation of T_0 and T_K observed under pressure is also understandable, since $T_0(P)$ can get close to $T_K(P)$ according to the parameters of \tilde{A} and n . The plot of $T_0(P)$ as well as $T_K(P)$ determined from the measurements of the specific heat and resistivity in Ce_7Ni_3 under pressure [48] enables us to estimate $\frac{1}{T_K}(\frac{\partial T_K}{\partial P}) = 4.0 \text{ GPa}^{-1}$, which is comparable to $\frac{1}{T_0}(\frac{\partial T_0}{\partial P})$ [39]. The bulk modulus is observed as $\kappa_T^{-1} = 24.6 \text{ GPa}$ at room temperature. The Grüneisen parameter is estimated to be $\Gamma \approx 100$ [39].

Figure 12 with the right-pointing P axis illustrates the T - P phase diagram of the Ce-based heavy electron systems. As P increases, the magnetic transition temperature T_c is suppressed to be absolute zero at the QCP denoted by P_c . At $P = P_c$, the magnetic susceptibility $\chi_Q(0, 0)$ diverges with $y = 0$ [see Eq. (21)]. Since y increases as P increases from P_c as shown by the dashed line, $(\frac{\partial y}{\partial P})_{T=0} > 0$ holds. [For the AFM QCP ($z = 2$) in $d = 2$, y starts to appear with zero slope $(\frac{\partial y}{\partial P})_{T=0} = 0$ at P_c , as discussed in Sec. VID.] Then, from Eq. (70) and the resultant Eq. (68), the positive thermal expansion coefficient appears $\alpha_{\text{mag}} > 0$ for $P > P_c$ at low temperatures.

This is understandable from the P dependence of the entropy S . When the QCP is approached from the paramagnetic side for $P > P_c$, $S/T \approx C_V/T$ (see Table I) increases toward P_c at the infinitesimal temperature. This gives $(\frac{\partial S}{\partial P})_T < 0$ for $P > P_c$, leading to $\alpha_{\text{mag}} > 0$ by Eq. (5) and hence $\Gamma_{\text{mag}} > 0$.

On the other hand, when P further decreases from P_c , the continuous transition to the magnetically ordered phase makes S/T decrease continuously for $P < P_c$ at the infinitesimal T . This gives $(\frac{\partial S}{\partial P})_T > 0$ for $P < P_c$, leading to $\alpha_{\text{mag}} < 0$ by Eq. (5) and hence $\Gamma_{\text{mag}} < 0$. Namely, the sign change of α_{mag} and Γ_{mag} occurs at P_c as a consequence of the entropy accumulation near the QCP [17,18]. It is noted that the sign change of α_{mag} was shown in Refs. [3,49] and the sign change of Γ_{mag} as well was discussed in Ref. [18].

2. Pressure effects on Yb-based systems

On the other hand, in the Yb-based heavy electron systems, the electronic state with $4f^{13}$ configuration for Yb^{3+} is understood on the basis of the hole picture. Hence, the f -hole level ε_f decreases as pressure increases in the Yb-based systems. In case this effect outweighs increase in the f - c hybridization, the Kondo coupling $J \sim \frac{V_{fc}^2}{\varepsilon_F - \varepsilon_f}$ decreases, giving rise to decrease in the Kondo temperature T_K under pressure. This yields $(\frac{\partial J}{\partial V})_S > 0$, which leads to $\Gamma_e < 0$ in Eq. (120) and hence the negative volume expansion $\alpha_e < 0$ in Eq. (117).

Namely, pressure induces the system where f electrons becomes more localized. When T_K decreases under pressure, decrease in the f -hole level is more effective than increase in the f - c hybridization, which makes v_F decrease. This effect contributes to the decrease in T_0 under pressure, i.e., $(\frac{\partial T_0}{\partial P}) < 0$. This yields negative thermal-expansion coefficient and Grüneisen parameter $\alpha_a < 0$ in Eq. (69) and $\Gamma_a < 0$ in Eq. (107).

Figure 12 with the left-pointing P axis illustrates the T - P phase diagram of the Yb-based heavy electron systems, where by applying pressure to the paramagnetic metal phase, the magnetic transition occurs at T_c starting from the QCP denoted by P_c . As P approaches P_c , the magnetic susceptibility $\chi_Q(0, 0) \propto y^{-1}$ increases and diverges at P_c for $T = 0$. Hence, $(\frac{\partial y}{\partial P})_T < 0$ holds for $P < P_c$, as shown by the dashed line. Thus, from Eq. (70), $\alpha_b < 0$ appears, which results in the negative thermal expansion coefficient $\alpha_{\text{mag}} < 0$ and hence $\Gamma_{\text{mag}} < 0$ for $P < P_c$ at low temperatures.

On the other hand, when P further increases from P_c , the continuous transition to the magnetically ordered phase makes S/T decrease continuously for $P > P_c$ at the infinitesimal T . This gives $(\frac{\partial S}{\partial P})_T < 0$ for $P > P_c$, leading to $\alpha_{\text{mag}} > 0$ by Eq. (5) and hence $\Gamma_{\text{mag}} > 0$. Namely, sign change of α_{mag} and Γ_{mag} occurs at P_c due to the entropy accumulation near the QCP.

D. Observation of α and Γ near the magnetic QCP

To detect the thermal expansion coefficient α and the Grüneisen parameter Γ near the QCP, experimental efforts have been devoted [16,51–53]. So far, a few data have been reported to exhibit the quantum criticality shown in Tables I and II in the stoichiometric compounds. To access the QCP, chemical doping has often been performed for high accuracy measurement of α at ambient pressure. However, the chemical doping more or less brings about effects of disorder, which sometimes masks true critical behaviors expected in clean systems. In this subsection, keeping this aspect in mind, experimental data to be compared with the criticality in Tables I and II are discussed.

In CeNi_2Ge_2 , the specific heat $C_{4f}/T \sim \gamma_0 - a_C T^{1/2}$ and resistivity $\rho \sim T^{n_\rho}$ ($1.2 \leq n_\rho \leq 1.5$) are observed in the low T region at ambient pressure, suggesting close proximity to the 3D AFM QCP (see Table I) [19]. The measured thermal expansion coefficient $\alpha = a_\alpha \sqrt{T} + b_\alpha T$ is in accordance with $\alpha_{\text{mag}} \sim T^{1/2}$ in Eq. (101) and $\alpha_c \sim T$ in Eq. (117). The Grüneisen parameter $\Gamma \approx 57$ at $T = 5$ K is already enhanced reflecting the contribution from Γ_a in Eq. (106) and the heavy-electron background as noted around Eq. (120). Further enhancement of Γ for lowering T is observed as $\Gamma \approx 98 \pm 10$ at $T \approx 0.1$ K, which suggests the contribution from Γ_b as shown in Eq. (109) (see Fig. 8).

As for the sign change of the thermal expansion coefficient, $\alpha_{\text{mag}} < 0$ in the AFM phase for $x < x_c$ and $\alpha_{\text{mag}} > 0$ in the paramagnetic phase for $x > x_c$ were observed in $\text{CeIn}_{3-x}\text{Sn}_x$ with $x_c = 0.67 \pm 0.03$ [20] and in $\text{CeRhIn}_{5-x}\text{Sn}_x$ with $x_c = 0.48$ [21].

Since the systematic study of $T_0(P)$ and $T_K(P)$ has already been performed in Ce_7Ni_3 [39,48], the measurements of $\alpha(T)$ and $\Gamma(T)$ at the QCP specified by $P_c = 0.39$ GPa and their

analyses based on Eqs. (68) and (106) are an interesting subject for future studies.

Furthermore, experimental observation of the quantum criticality shown in Tables I and II for each class is also greatly desired. Near the FM QCP, $(\frac{\partial y}{\partial P})_T$ can be directly observed by measuring the pressure dependence of the uniform susceptibility since $\chi_0(0, 0)^{-1} \propto y$ holds. Near the AFM QCP, by measuring the pressure dependence of the NMR relaxation rate $(T_1 T)^{-1}$ or resistivity $\rho(T)$ at low temperatures, $(\frac{\partial y}{\partial P})_T$ can be extracted [3,25]. Observation of $T_0(P)$ as well as $T_K(P)$ and evaluation of $\frac{1}{T_0}(\frac{\partial T_0}{\partial P})_T$ as done in Ce_7Ni_3 and $(\frac{\partial y}{\partial P})_T$ enables us to make the complete analysis of $\alpha(T)$ and $\Gamma(T)$ at the QCP on the basis of Eqs. (68) and (106). Such measurements are much to be desired.

X. SUMMARY

The properties of the thermal-expansion coefficient α and the Grüneisen parameter Γ near the magnetic QCP in itinerant electron systems have been discussed on the basis of the SCR theory in this paper.

By taking into account the zero point as well as thermal spin fluctuation, we have calculated the specific heat C_V at the magnetic QCP by considering the stationary condition of the SCR theory correctly. For each class of the FM QCP ($z = 3$) and AFM QCP ($z = 2$) in $d = 3$ and 2, C_V was shown to be expressed as $C_V = C_a - C_b$, where C_a is dominant for $t \ll 1$. The criticality of C_a reproduces the results obtained by the past SCR theory, which was endorsed by the RG theory.

Then we have derived the thermal-expansion coefficient α starting from the expression of the entropy in the SCR theory, which has been proven to be equivalent to α derived from the expression of the free energy in the SCR theory. The result shows that α is expressed as $\alpha = \alpha_a + \alpha_b$ with $\alpha_a = \frac{1}{V} \frac{C_a}{T_0} (\frac{\partial T_0}{\partial P})_T$ and $\alpha_b = \frac{1}{V} \frac{C_b}{t} (\frac{\partial y}{\partial P})_T$ where α_b is dominant for $t \ll 1$. An important result is that α_b contains the temperature-dependent $(\frac{\partial y}{\partial P})_T$, which contributes to the crossover from the quantum-critical to Curie-Weiss regimes for each universality class and even affects the critical behavior for $t \ll 1$ in the case of upper critical dimension, i.e., $z = 2$ in $d = 2$.

On the basis of these correctly calculated C_V and α , we have derived the Grüneisen parameter Γ . The results show that Γ is expressed as $\Gamma = \Gamma_a + \Gamma_b$, where Γ_a and Γ_b contain α_a and α_b , respectively. For $t \ll 1$, Γ_a is given by $\Gamma_a = -\frac{V}{T_0} (\frac{\partial T_0}{\partial P})_T$, which has an enhanced value of typically $O(10)$ in the heavy electron systems. A remarkable result is that for $t \ll 1$, Γ_b is expressed as $\Gamma_b = -\frac{C_b}{C_a} \frac{V}{t} (\frac{\partial y}{\partial P})_T$, which diverges at the QCP for each universality class. This result shows that the inverse susceptibility (renormalized by the mode-mode coupling of spin fluctuations) coupled to V gives rise to the divergence of the Grüneisen parameter even though the characteristic energy scale T_0 remains finite at the QCP.

The obtained results give the complete expressions of α and Γ , which consist of not only the critical part but also non-critical part with their coefficients as well as the temperature dependencies. The temperature dependencies of α_b and Γ_b for $t \ll 1$ coincide with the critical parts shown by the RG theory for each universality class except for the case $z = 2$ in $d = 2$, where the temperature dependent $(\frac{\partial y}{\partial P})_T$ affects the criticality. The complete expressions of α and Γ clarify their whole

temperature dependencies from the quantum-critical regime to the Curie-Weiss regime, and are useful for comparison with experiments. The temperature dependence of α coincides with the Moriya-Usami theory for $t \ll 1$ where $\alpha \propto \frac{dy}{dt}$ holds for $d + z > 4$ and approximately holds for $d + z = 4$.

Our study has made it possible to evaluate the temperature dependence of the Grüneisen parameter in the Curie-Weiss regime. The results are $\Gamma(T) \sim T^{-0.43}$ for the $d = 3$ FM and AFM QCPs, $\Gamma(T) \sim T^{-0.50}$ for the $d = 2$ FM QCP, and $\Gamma(T) \sim T^{-0.41}$ for the $d = 2$ AFM QCP. These results are also useful for comparison with experiments.

In the heavy electron systems, the Grüneisen parameter in the Fermi-liquid regime is shown to be enhanced by a factor of $(JN_{\text{cF}})^{-1} \gg 1$, where J is the Kondo coupling and N_{cF} is the density of states of conduction electrons at the Fermi level. When the QCP is approached, further enhancement caused by spin fluctuation is added to the heavy-electron background, and Γ eventually diverges at the QCP.

The characteristic temperature of spin fluctuation is shown to be proportional to the Kondo temperature in the lattice system $T_0 \propto T_{\text{K}}$. At sufficiently low temperatures, $\alpha > 0$ and $\Gamma > 0$ appear in the paramagnetic phase for $P > P_{\text{c}}$, while $\alpha < 0$ and $\Gamma < 0$ appear in the magnetically ordered phase for $P < P_{\text{c}}$ in the Ce-based heavy electron systems. On the other hand, $\alpha < 0$ and $\Gamma < 0$ appear in the paramagnetic phase for $P < P_{\text{c}}$, while $\alpha > 0$ and $\Gamma > 0$ appear in the magnetically ordered phase for $P > P_{\text{c}}$ in the Yb-based heavy electron systems.

ACKNOWLEDGMENTS

We thank K. Umeo for informative discussions on the experimental data of Ce_7Ni_3 . This work was supported by JSPS KAKENHI Grant Numbers JP15K05177, JP16H01077, JP18H04326, JP18K03542, and JP17K05555.

APPENDIX A: GRÜNEISEN PARAMETER IN FERMILIQUID AT LOW TEMPERATURES

In this Appendix it is shown that the Grüneisen parameter for free electrons in the isotropic three-dimensional system is easily derived from the specific heat at low temperatures.

At low temperatures, the specific heat at a constant volume is given by

$$C_V = Nk_{\text{B}} \frac{\pi^2}{2} \frac{T}{T_{\text{F}}} = Nk_{\text{B}} \frac{T}{T^*}, \quad (\text{A1})$$

where T^* is defined as $T^* \equiv \frac{2}{\pi^2} T_{\text{F}}$. Then, the entropy S is given by

$$S = \int_0^T \frac{C_V}{T} dT = Nk_{\text{B}} \frac{T}{T^*}. \quad (\text{A2})$$

Note that the Fermi temperature T_{F} is expressed as $T_{\text{F}} = \frac{\varepsilon_{\text{F}}}{k_{\text{B}}}$ with the Fermi energy $\varepsilon_{\text{F}} \equiv \frac{\hbar^2 k_{\text{F}}^2}{2m}$, where m and k_{F} are mass of an electron and the Fermi wave number $k_{\text{F}} = (3\pi^2 \frac{N_{\text{c}}}{V})^{1/3}$, respectively. Then, by differentiating Eq. (A2) with respect to the volume V under a constant entropy S , we obtain

$$\left(\frac{\partial T^*}{\partial V} \right)_S = -\frac{2}{3} \frac{T^*}{V}. \quad (\text{A3})$$

Hence, by Eq. (10), the Grüneisen parameter Γ is obtained as

$$\Gamma = \frac{2}{3}, \quad (\text{A4})$$

which reproduces the result of the free-electron model [37].

APPENDIX B: QUANTUM CRITICALITY IN $d = 3$

In this Appendix it is explained that the quantum criticality at the QCP in $d = 3$ is given by Eq. (38) by analyzing the solution of the SCR equation [Eq. (33)] at low temperatures [26]. The x integral on the r.h.s. of Eq. (33) is defined by Eq. (82) as

$$L \equiv \int_0^{x_{\text{c}}} dx x^{d+z-3} \left\{ \ln u - \frac{1}{2u} - \psi(u) \right\}, \quad (\text{B1})$$

where d is the spatial dimension and z is the dynamical exponent. By changing the integral variable as $x' = x/t^{1/z}$, Eq. (B1) is expressed as

$$L = t^{\frac{d+z-2}{z}} \int_0^{\frac{x_{\text{c}}}{t^{1/z}}} dx' (x')^{d+z-3} \left\{ \ln u - \frac{1}{2u} - \psi(u) \right\}, \quad (\text{B2})$$

where u is given by

$$u = (x')^{z-2} \left\{ \frac{y}{t^{z/2}} + (x')^2 \right\}. \quad (\text{B3})$$

We see that at low temperatures $t \ll 1$ for

$$\frac{y}{t^{z/2}} \rightarrow 0, \quad (\text{B4})$$

the x' integral in $d = 3$ converges in Eq. (B2) where the upper bound of the integral is set to be ∞ . Hence, the t dependence of L is evaluated as

$$L \propto t^{\frac{z+1}{z}}. \quad (\text{B5})$$

Then, from the SCR equation [Eq. (33)], the following solution

$$y \propto t^{\frac{z+1}{z}} \quad (\text{B6})$$

is immediately obtained at the QCP where $y_0 = 0.0$ is set in Eq. (33). It is confirmed that this result satisfies the condition of Eq. (B4), i.e., $y/t^{z/2} \ll 1$, for $t \ll 1$.

APPENDIX C: SOLUTION OF SCR EQUATION FOR $z = 3$ in $d = 2$

The derivation of the solution of the SCR equation [Eq. (33)] for $z = 3$ in $d = 2$ is shown in this Appendix [10].

By using the approximation formula

$$\ln u - \frac{1}{2u} - \psi(u) \approx \frac{1}{2u(1+6u)} \quad (\text{C1})$$

in Eq. (B1), the x integration can be performed and the leading terms are evaluated as

$$L \approx \frac{t}{4} \ln \left[\frac{1}{y} \left(\frac{t}{6} \right)^{2/3} \right], \quad (\text{C2})$$

for $y \ll t^{2/3} \ll 1$. Then, the solution of the SCR equation [Eq. (33)] $y = y_0 + y_1 L$ at the QCP with $y_0 = 0.0$ is obtained

as follows:

$$y = -\frac{y_1}{12} t \ln t. \quad (\text{C3})$$

Since the correlation length ξ is given by $y \propto \xi^{-2}$, this coincides with the result of the RG theory for $z = 3$ in $d = 2$ in Ref. [8].

APPENDIX D: EQUIVALENCE OF SCR SOLUTION AND RENORMALIZATION GROUP FOR $z = 2$ IN $d = 2$

In this Appendix it is shown that the solution of the SCR equation [Eq. (34)] for $z = 2$ in $d = 2$ coincides with the result of the RG theory by Millis [8].

By using the approximation formula Eq. (C1) in the SCR equation [Eq. (34)], the x integration can be performed as

$$y = y_0 + \frac{y_1}{2} \left(y \ln y + \frac{t}{2} \left[\ln \frac{x_c^2 + y}{y} - \ln \frac{x_c^2 + y + \frac{t}{6}}{y + \frac{t}{6}} \right] \right). \quad (\text{D1})$$

At the QCP with $y_0 = 0.0$, the leading terms are evaluated as

$$-\ln 2y \approx \frac{t}{2y} \ln \frac{t}{2y}, \quad (\text{D2})$$

for $y \ll t \ll 1$. Then, one finds that

$$y = -t \frac{\ln(-\ln t)}{2 \ln t} \quad (\text{D3})$$

is the solution of Eq. (D2) up to the order of $\ln t$, which coincides with the result of the RG theory for $z = 2$ in $d = 2$ in Ref. [8].

APPENDIX E: DERIVATION OF EQ. (72)

In this Appendix the derivation of Eq. (72) is explained.

By differentiating the free energy in the SCR theory [Eq. (22)] with respect to V under a constant temperature, we obtain

$$\begin{aligned} \left(\frac{\partial \tilde{F}}{\partial V} \right)_T &= \frac{1}{\pi} \sum_q \int_0^{\omega_c} d\omega \left[\frac{\partial}{\partial \Gamma_q} \left(\frac{\Gamma_q}{\omega^2 + \Gamma_q^2} \right) \right]_T \left(\frac{\partial \Gamma_q}{\partial V} \right)_T \left[\frac{\omega}{2} + T \ln(1 - e^{-\frac{\omega}{T}}) \right] - \frac{1}{2N_F} \left(\frac{\partial \eta}{\partial V} \right)_T \langle \varphi^2 \rangle_{\text{eff}} \\ &+ \left[\frac{\eta_0 - \eta}{2N_F} + \frac{6v_4}{N} \langle \varphi^2 \rangle_{\text{eff}} \right] \left(\frac{\partial \langle \varphi^2 \rangle_{\text{eff}}}{\partial V} \right)_T + \left\{ \left(\frac{\partial \eta_0}{\partial V} \right)_T \frac{1}{2N_F} + (\eta_0 - \eta) \left[\frac{\partial}{\partial V} \left(\frac{1}{2N_F} \right) \right]_T \right\} \langle \varphi^2 \rangle_{\text{eff}} + \frac{3}{N} \left(\frac{\partial v_4}{\partial V} \right)_T \langle \varphi^2 \rangle_{\text{eff}}^2. \end{aligned} \quad (\text{E1})$$

Since the second term of Eq. (71) is expressed as $(\partial \Gamma_q / \partial y)_T (\partial y / \partial V)_T$, by substituting

$$\left(\frac{\partial \eta}{\partial V} \right)_T = A q_B^2 \left(\frac{\partial y}{\partial V} \right)_T + y \left[\frac{\partial (A q_B^2)}{\partial V} \right]_T \quad (\text{E2})$$

into the second term of Eq. (E1), the first and second terms of Eq. (E1) are expressed as

$$\begin{aligned} \frac{1}{T_0} \left(\frac{\partial T_0}{\partial V} \right)_T I + \left\{ \frac{1}{\pi} \sum_q \int_0^{\omega_c} d\omega \left[\frac{\partial}{\partial \Gamma_q} \left(\frac{\Gamma_q}{\omega^2 + \Gamma_q^2} \right) \right]_T \left(\frac{\partial \Gamma_q}{\partial y} \right)_T \left[\frac{\omega}{2} + T \ln(1 - e^{-\frac{\omega}{T}}) \right] - T_A \langle \varphi^2 \rangle_{\text{eff}} \right\} \left(\frac{\partial y}{\partial V} \right)_T \\ - y \left[\frac{\partial (A q_B^2)}{\partial V} \right]_T \frac{1}{2N_F} \langle \varphi^2 \rangle_{\text{eff}}, \end{aligned} \quad (\text{E3})$$

where I is defined by Eq. (73) and the definition of T_A [Eq. (27)] has been used. Here we note that the $\{\dots\}$ part vanishes because of the stationary condition $(\partial \tilde{F} / \partial y)_T = 0$ applied to

$$\left(\frac{\partial \tilde{F}}{\partial V} \right)_T = \left(\frac{\partial y}{\partial V} \right)_T \left(\frac{\partial \tilde{F}}{\partial y} \right)_T + \dots \quad (\text{E4})$$

This implies that the coefficient multiplied to $(\partial y / \partial V)_T$ in the calculation of $(\partial \tilde{F} / \partial V)_T$ vanishes, which is nothing but the $\{\dots\}$ part in Eq. (E3). This can also be directly confirmed by noting the fact that the term in the second line of Eq. (E3) equals to $(\partial F_{\text{eff}} / \partial y)_T$, which is expressed as

$$\left(\frac{\partial F_{\text{eff}}}{\partial y} \right)_T = A q_B^2 \frac{T}{2} \sum_q \sum_l \frac{1}{\eta + A q^2 + C_q |\omega_l|} = T_A \langle \varphi^2 \rangle_{\text{eff}}. \quad (\text{E5})$$

Here F_{eff} was defined by Eq. (15) and the definition of $\langle \varphi^2 \rangle_{\text{eff}}$ [Eq. (17)] has been used to derive the last result. Then, the last term inside of $\{\dots\}$ in Eq. (E3) is subtracted from Eq. (E5), which results in zero.

On the first term in the second line of Eq. (E1), the $[\dots]$ part multiplied to $(\partial\langle\varphi^2\rangle_{\text{eff}}/\partial V)_T$ vanishes because of the SCR equation [Eq. (16)].

On the second term in the second line of Eq. (E1), the $\{\dots\}$ part is expressed as

$$\left(\frac{\partial\eta_0}{\partial V}\right)_T \frac{1}{2N_F} + (\eta_0 - \eta) \left[\frac{\partial}{\partial V} \left(\frac{1}{2N_F} \right) \right]_T = \left[\frac{\partial}{\partial V} \left(\frac{\eta_0}{Aq_B^2} \right) \right]_T T_A + \left(\frac{\eta_0}{Aq_B^2} - y \right) \left(\frac{\partial T_A}{\partial V} \right)_T + y \left[\frac{\partial(Aq_B^2)}{\partial V} \right]_T \frac{1}{2N_F}. \quad (\text{E6})$$

Then, it turns out that the contribution from the last term is canceled by the last term of Eq. (E3).

Eventually, the remaining terms are the first term of Eq. (E3), the contributions from the first and second terms on the r.h.s. of Eq. (E6), and the last term of Eq. (E1), which result in Eq. (72).

APPENDIX F: DERIVATION OF THE LAST THREE TERMS IN EQ. (83)

In this Appendix the last three terms in Eq. (83) are derived from the last three terms in Eq. (79).

The last three terms in Eq. (79) are calculated by using the SCR equation [Eq. (16)], as follows:

$$-\frac{\partial}{\partial T} \left\{ \left[\frac{\partial}{\partial V} \left(\frac{\eta_0}{Aq_B^2} \right) \right]_T T_A \langle\varphi^2\rangle_{\text{eff}} \right\} \Big|_V = - \left(\frac{\partial y}{\partial t} \right)_V \frac{N}{6v_4} \frac{T_A^2}{T_0} \left[\frac{\partial}{\partial V} \left(\frac{\eta_0}{Aq_B^2} \right) \right]_T, \quad (\text{F1})$$

$$-\frac{\partial}{\partial T} \left[\left(\frac{\eta_0}{Aq_B^2} - y \right) \left(\frac{\partial T_A}{\partial V} \right)_T \langle\varphi^2\rangle_{\text{eff}} \right] \Big|_V = \left(\frac{\partial y}{\partial t} \right)_V \frac{2}{T_0} \langle\varphi^2\rangle_{\text{eff}} \left(\frac{\partial T_A}{\partial V} \right)_T, \quad (\text{F2})$$

$$-\frac{\partial}{\partial T} \left[\frac{3}{N} \left(\frac{\partial v_4}{\partial V} \right)_T \langle\varphi^2\rangle_{\text{eff}}^2 \right] \Big|_V = - \left(\frac{\partial y}{\partial t} \right)_V \frac{T_A}{T_0} \langle\varphi^2\rangle_{\text{eff}} \frac{1}{v_4} \left(\frac{\partial v_4}{\partial V} \right)_T. \quad (\text{F3})$$

These are the last three terms in Eq. (83), respectively.

APPENDIX G: DERIVATION OF EQ. (86)

The derivation of Eq. (86) is shown in this Appendix.

The pressure dependence of C_1 and C_2 appears via the characteristic temperature T_0 , as seen in Eqs. (28) and (29), respectively. Hence, differentiation of C_1 and C_2 with respect to the pressure P under a constant temperature gives

$$\left(\frac{\partial C_1}{\partial P} \right)_T = - \frac{2}{T_0} \left(\frac{\partial T_0}{\partial P} \right)_T \int_0^{x_c} dx x^{d+z-3} \frac{\omega_{cT_0}^2}{\omega_{cT_0}^2 + x^{2z}}, \quad (\text{G1})$$

$$\left(\frac{\partial C_2}{\partial P} \right)_T = - \frac{4}{T_0} \left(\frac{\partial T_0}{\partial P} \right)_T \int_0^{x_c} dx x^{d+z-5} \frac{\omega_{cT_0}^2 x^{2z}}{(\omega_{cT_0}^2 + x^{2z})^2}, \quad (\text{G2})$$

respectively.

Near the QCP, the second term in $\{\dots\}$ of Eq. (80) can be expanded around $y = 0$ as

$$\int_0^{x_c} dx x^{d+z-3} \frac{\omega_{cT}^2}{\omega_{cT}^2 + u^2} = \int_0^{x_c} dx x^{d+z-3} \frac{\omega_{cT_0}^2}{\omega_{cT_0}^2 + x^{2z}} - 2 \int_0^{x_c} dx x^{d+z-5} \frac{\omega_{cT_0}^2 x^{2z}}{(\omega_{cT_0}^2 + x^{2z})^2} y + \dots \quad (\text{G3})$$

By substituting Eqs. (G1) and (G2) into the first and second terms on the r.h.s. of Eq. (G3), respectively, we obtain

$$-\frac{1}{T_0} \left(\frac{\partial T_0}{\partial P} \right)_T \int_0^{x_c} dx x^{d+z-3} \frac{\omega_{cT}^2}{\omega_{cT}^2 + u^2} = \frac{1}{2} \left\{ \left(\frac{\partial C_1}{\partial P} \right)_T - \left(\frac{\partial C_2}{\partial P} \right)_T y \right\} + \dots \quad (\text{G4})$$

for small y , which holds near the QCP. This gives Eq. (86).

APPENDIX H: DERIVATION OF EQ. (87)

The derivation of Eq. (87) is explained in this Appendix.

By substituting Eq. (85) and Eq. (86) into the third term and the fourth term in $\{\dots\}$ in the first line of Eq. (84), respectively, the terms with $\{\dots\}$ in the first line of Eq. (84) are expressed as

$$\begin{aligned} & \frac{1}{V} \left(\frac{\partial y}{\partial t} \right)_V \left[- \frac{1}{T_0} \left(\frac{\partial T_0}{\partial P} \right)_T \tilde{C}_b + \frac{Nd}{2} \left\{ \frac{1}{T_0} \left(\frac{\partial T_0}{\partial P} \right)_T (C_1 - C_2 y_0) + \left(\frac{\partial C_1}{\partial P} \right)_T - \left(\frac{\partial C_2}{\partial P} \right)_T y_0 \right. \right. \\ & \left. \left. + \left[\frac{1}{T_0} \left(\frac{\partial T_0}{\partial P} \right)_T \left(2 - C_2 y_1 \frac{d}{2} \right) - \left(\frac{\partial C_2}{\partial P} \right)_T y_1 \frac{d}{2} \right] L \right\} \right], \end{aligned} \quad (\text{H1})$$

where the SCR equation (33), which is written as $y = y_0 + (d/2)y_1 L$ using the definition of L [Eq. (82)], is substituted into y on the r.h.s. of Eqs. (85) and (86).

Then, one realizes that the first line except for the \tilde{C}_b term inside the outermost $[\dots]$ in Eq. (H1) can be expressed in the form as

$$N \frac{2}{y_1} \left(\frac{\partial y_0}{\partial P} \right)_T, \quad (\text{H2})$$

as far as the terms with the pressure derivative of T_0 , C_1 , and C_2 in Eq. (88) are concerned. Similarly, one realizes that the second line inside the outermost $[\dots]$ in Eq. (H1) can be expressed in the form as

$$N \frac{d}{y_1} \left(\frac{\partial y_1}{\partial P} \right)_T L, \quad (\text{H3})$$

as far as the terms with the pressure derivative of T_0 , C_1 , and C_2 in Eq. (89) are concerned.

As for the last two terms in Eq. (84), it turns out that the terms other than noted above in Eqs. (88) and (89) complement the remaining terms in $(\partial y_0/\partial P)_T$ in Eq. (H2) and $(\partial y_1/\partial P)_T$ in Eq. (H3), respectively, as follows:

The term with $[\partial(\eta_0/Aq_B^2)/\partial P]_T$ in Eq. (84) can be expressed in the form as Eq. (H2), as far as the term with the pressure derivative of $\eta_0/(Aq_B^2)$ in Eq. (88) is concerned.

On the term with $(\partial T_A/\partial P)_T$ in Eq. (84), by substituting Eqs. (26) and (30) into the expression of $\langle \varphi^2 \rangle_{\text{eff}}$ [Eq. (18)] and using the SCR equation [Eq. (33)], we obtain

$$-\frac{2}{T_0} \langle \varphi^2 \rangle_{\text{eff}} \left(\frac{\partial T_A}{\partial P} \right)_T = -Nd \frac{1}{T_A} \left(\frac{\partial T_A}{\partial P} \right)_T \left[C_1 - C_2 y_0 + \left(2 - C_2 y_1 \frac{d}{2} \right) L \right]. \quad (\text{H4})$$

On the last term in Eq. (84), we similarly obtain

$$\frac{T_A}{T_0} \langle \varphi^2 \rangle_{\text{eff}} \frac{1}{v_4} \left(\frac{\partial v_4}{\partial P} \right)_T = \frac{Nd}{2} \frac{1}{v_4} \left(\frac{\partial v_4}{\partial P} \right)_T \left[C_1 - C_2 y_0 + \left(2 - C_2 y_1 \frac{d}{2} \right) L \right]. \quad (\text{H5})$$

Hence, the last two terms in Eq. (84) can be expressed in the form as the summation of Eqs. (H2) and (H3), as far as the terms with the pressure derivative of T_A and v_4 in Eqs. (88) and (89), respectively, are concerned.

Thus, the summation of all these terms noted above lead to the summation of Eqs. (H2) and (H3), which is nothing but the last two terms of Eq. (87). Since the first term with C_a and the third term with \tilde{C}_b in Eq. (84) directly appear in Eq. (87) as the first and second terms, respectively, by combining the result of the last two terms of Eq. (87) derived above, we obtain Eq. (87).

-
- [1] T. Moriya and A. Kawabata, *J. Phys. Soc. Jpn.* **34**, 639 (1973).
[2] T. Moriya and A. Kawabata, *J. Phys. Soc. Jpn.* **35**, 669 (1973).
[3] T. Moriya, *Spin Fluctuations in Itinerant Electron Magnetism* (Springer, Berlin, 1985).
[4] G. G. Lonzarich and L. Taillefer, *J. Phys. C* **18**, 4339 (1985).
[5] K. Makoshi and T. Moriya, *J. Phys. Soc. Jpn.* **38**, 10 (1975).
[6] K. Ueda and T. Moriya, *J. Phys. Soc. Jpn.* **39**, 605 (1975).
[7] J. A. Hertz, *Phys. Rev. B* **14**, 1165 (1976).
[8] A. J. Millis, *Phys. Rev. B* **48**, 7183 (1993); the statement ‘‘SCR procedure does not yield the log corrections in $d = 2$ for $z = 3$ and $z = 2$.’’ is not correct. The SCR results coincide with those derived by the renormalization group theory including the log corrections in $d = 2$ for $z = 3$ [10] and $z = 2$ (T. Moriya, private communications). See, for details, Appendixes C and D in the present paper, respectively.
[9] U. Zülicke and A. J. Millis, *Phys. Rev. B* **51**, 8996 (1995).
[10] M. Hatatani and T. Moriya, *J. Phys. Soc. Jpn.* **64**, 3434 (1995).
[11] T. Moriya and T. Takimoto, *J. Phys. Soc. Jpn.* **64**, 960 (1995).
[12] A. Ishigaki and T. Moriya, *J. Phys. Soc. Jpn.* **65**, 376 (1996).
[13] A. Ishigaki and T. Moriya, *J. Phys. Soc. Jpn.* **67**, 3924 (1998).
[14] A. Ishigaki and T. Moriya, *J. Phys. Soc. Jpn.* **68**, 3673 (1999).
[15] T. Moriya and K. Usami, *Solid State Commun.* **34**, 95 (1980).
[16] S. Kambe, J. Flouquet, P. Lejay, P. Haen, and A. de Visser, *J. Phys.: Condens. Matter* **9**, 4917 (1997).
[17] L. Zhu, M. Garst, A. Rosch, and Q. Si, *Phys. Rev. Lett.* **91**, 066404 (2003).
[18] M. Garst and A. Rosch, *Phys. Rev. B* **72**, 205129 (2005).
[19] R. Küchler, N. Oeschler, P. Gegenwart, T. Cichorek, K. Neumaier, O. Tegus, C. Geibel, J. A. Mydosh, F. Steglich, L. Zhu, and Q. Si, *Phys. Rev. Lett.* **91**, 066405 (2003).
[20] R. Küchler, P. Gegenwart, J. Custers, O. Stockert, N. Caroca-Canales, C. Geibel, J. G. Sereni, and F. Steglich, *Phys. Rev. Lett.* **96**, 256403 (2006).
[21] J. G. Donath, F. Steglich, E. D. Bauer, F. Ronning, J. L. Sarrao, and P. Gegenwart, *Europhys. Lett.* **87**, 57011 (2009).
[22] E. Grüneisen, *Ann. Phys.* **344**, 257 (1912).
[23] R. Takke, M. Nicksch, W. Assmus, B. Luthi, R. Pott, R. Schefzyk, and D. K. Wohlleben, *Z. Phys. B* **44**, 33 (1981).
[24] P. Thalmeier and P. Fulde, *Europhys. Lett.* **1**, 367 (1986).
[25] T. Moriya and K. Ueda, *Rep. Prog. Phys.* **66**, 1299 (2003).
[26] T. Moriya, *Jisei Butsurigaku* (Asakura, Tokyo, 2006) [in Japanese].
[27] Y. Takahashi, *J. Phys.: Condens. Matter* **11**, 6439 (1999).
[28] Y. Takahashi and H. Nakano, *J. Phys.: Condens. Matter* **18**, 521 (2006).
[29] J. Flouquet, *Progress in Low Temperature Physics*, edited by W. P. Halperin (Elsevier, Amsterdam, 2005), Vol. 15, p. 139.
[30] We employ Eq. (11) which essentially describes isotropic spin space, i.e., Heisenberg symmetry. It is noted that the action with the factor 3 multiplied to the r.h.s. of Eq. (11) corresponds to the case for Heisenberg symmetry discussed in Ref. [14] and Refs. [27,31].

- [31] It is straightforward to extend the present results to the case of magnetic fluctuations of XY or Heisenberg type, where the factor of 2 or 3 is multiplied to the free energy in Eq. (22), respectively (note that the solution of the SCR equation correctly satisfies the Mermin-Wagner theorem for the Heisenberg symmetry as shown in Fig. 1). Hence, the factor is also to be multiplied to the entropy in Eq. (39) and the specific heat in Eqs. (41) and (43). In real materials, there exists more or less anisotropy of the spin space, leading to anisotropic spin fluctuation. Therefore, we plot α as well as C_V for a single component of the spin fluctuation with the factor of 1 in a series of figures for convenience of comparison with experiments. As for the Grüneisen parameter Γ , the results shown in Figs. 7–10 are not affected by this factor except for κ_T , since the factors in α and C_V canceled each other in Eq. (107).
- [32] R. P. Feynman, *Statistical Mechanics* (Addison-Wesley, Reading, MA, 1990), Sect. 3.4.
- [33] N. D. Mermin and H. Wagner, *Phys. Rev. Lett.* **17**, 1307 (1966).
- [34] M. Hatatani, O. Narikiyo, and K. Miyake, *J. Phys. Soc. Jpn.* **67**, 4002 (1998); M. Hatatani, Ph.D. thesis, Graduate School of Engineering Science, Osaka University, 2000.
- [35] Although the criticality in $d = 2$ for $z = 2$, $y \sim -\frac{t}{\ln t}$ was reported in Ref. [13], more precisely it can be shown that $y \sim -t \frac{\ln(-\ln t)}{\ln t}$ is the solution of the SCR equation, which coincides with the result of the renormalization group discussed in Ref. [8] (see Appendix D).
- [36] In the RG theory it was reported that the additional log correction to the one reported in Ref. [17] appears in $d = 2$ and $z = 2$ (see p. 53 of <http://www.thp.uni-koeln.de/rosch/documents/DrArbeitMarkusGarst.pdf>). In the infinite limit of the number of the components, the additional log terms are $\ln(-T)$ in α and $\ln(-T)$ in Γ , which are to be compared with our results, $\ln(-\frac{T}{\ln T})$ and $\ln(-\frac{T}{\ln T})$ in Table II, respectively.
- [37] N. W. Ashcroft and N. D. Mermin, *Solid State Physics* (Saunders College, Philadelphia, 1976).
- [38] A. V. Goltsev and M. M. Abd-Elmeguid, *J. Phys.: Condens. Matter* **17**, S813 (2005).
- [39] K. Umeo, H. Kadomatsu, and T. Takabatake, *Phys. Rev. B* **54**, 1194 (1996).
- [40] Y. Ōno, T. Matsuura, and Y. Kuroda, *Physica C (Amsterdam)* **159**, 878 (1989).
- [41] N. Shibata, T. Nishino, K. Ueda, and C. Ishii, *Phys. Rev. B* **53**, R8828 (1996).
- [42] J. D. Thompson, J. M. Lawrence, and Z. Fisk, *J. Low Temp. Phys.* **95**, 59 (1994).
- [43] A. de Visser, J. N. M. Franse, and J. Flouquet, *Physica B (Amsterdam)* **161**, 324 (1989).
- [44] It is generally expected that the first term in Eq. (120) dominates over the second term since the volume dependence of the Kondo exchange coupling is much stronger than that of the density of states of conduction electrons. If we adopt the tight-binding picture with the distance dependence of the hybridization between the f and conduction electrons $V_{fc} \sim 1/r^{\ell+\ell'+1}$ with the azimuthal quantum numbers $\ell = 3$, ℓ' , respectively [45–47], we estimate $\frac{V}{J}(\frac{\partial J}{\partial V}) \sim -\frac{1}{d}[2\ell' + 6 + O(\frac{\epsilon_f}{\epsilon_F - \epsilon_f})]$ in the d -dimensional system. The absolute value is larger than $c \equiv \frac{V}{N_F}(\frac{\partial N_F}{\partial V}) \sim \frac{2}{d}$ estimated from the nearly free-electron picture, since ϵ_f is not so close to ϵ_F in typical heavy-electron systems. This reflects the fact that the locality of the $4f$ wave function reacts severely to the volume change of the system.
- [45] O. K. Andersen and O. Jepsen, *Physica B (Amsterdam)* **91**, 317 (1977).
- [46] O. K. Andersen, W. Klose, and H. Nohl, *Phys. Rev. B* **17**, 1209 (1978).
- [47] W. A. Harrison, *Electronic Structure and the Properties of Solids* (W. H. Freeman, San Francisco, CA, 1980).
- [48] K. Umeo, H. Kadomatsu, and T. Takabatake, *J. Phys.: Condens. Matter* **8**, 9743 (1996).
- [49] It should be noted that sign change of α_{mag} in the ferromagnetically ordered phase ($\alpha_{\text{mag}} < 0$) and the paramagnetic phase ($\alpha_{\text{mag}} > 0$) was shown by the Moriya-Usami theory [15] to explain the observation in ZrZn₂ [50]. See Fig. 5.4 on p. 89 in Sect. 5.2 in Ref. [3].
- [50] S. Ogawa and N. Kasai, *J. Phys. Soc. Jpn.* **27**, 789 (1969).
- [51] R. KÜchler, P. Gegenwart, C. Geibel, and F. Steglich, *Sci. Technol. Adv. Mater.* **8**, 428 (2007), and references therein.
- [52] A. Steppke, R. Kuchler, S. Lausberg, E. Lengyel, L. Steinke, R. Borth, T. Luhmann, C. Krellner, M. Nicklas, C. Geibel, F. Steglich, and M. Brando, *Science* **339**, 933 (2013).
- [53] P. Gegenwart, *Rep. Prog. Phys.* **79**, 114502 (2016), and references therein.